Solar Energy 271 (2024) 112420

Contents lists available at ScienceDirect

Solar Energy

journal homepage: www.elsevier.com/locate/solener

Technical and economic study of solar energy concentration technologies (linear Fresnel and parabolic trough collectors) to generate process heat at medium temperature for the dairy industry of Spain

Rubén Rodríguez Rodrigo [a,*], Ricardo Díaz Martín [b], Marcos Baranda Fernández [c], Jesús Ángel Román Gallego [d], Carlos Mayo del Río [e]

[a] Zamora Higher Polytechnic School, Construction and Agronomy Department, Universidad de Salamanca, Requejo Avenue, 33, 49029 Zamora, Spain
[b] Higher Polytechnic School, Universidad CEU-San Pablo, Montepríncipe Avenue, no. 28668 Boadilla del Monte, Madrid, Spain
[c] Chemical and Materials Engineering Department, Universidad Complutense de Madrid, Sciencie Square, 2, 28040 Madrid, Spain
[d] Zamora Higher Polytechnic School, Informatics and Automation Department, Universidad de Salamanca, Requejo Avenue, 33, 49029 Zamora, Spain
[e] Surface Engineering and Nanostructural Materials Research Groups Chemical and Materials Engineering Department, Faculty of Chemical Sciences, Universidad Complutense de Madrid, Sciencie Square, 2, 28040 Madrid, Spain

ARTICLE INFO

Keywords:
Solar heat for industrial processes
Solar thermal energy
Solar concentration technologies
Thermal energy generation cost
Dairy industry
SHIP systems integration

ABSTRACT

Real energy consumption data were taken from the 17 most important companies of the dairy industry distributed across different Spanish geographical locations, studying the technical and economic feasibility of integrating solar concentration technologies suitable for the required thermal level of medium temperature in that industrial sector. The results show that the percentage of use of available thermal energy (%U) and the size of the solar plant, in addition to many other variables such as location, are decisive parameters for determining the cost of generating thermal energy and comparing it with the cost of conventional energies (natural gas, diesel and fuel oil). A 20-year time horizon is considered and three different scenarios are taken into account as regards the price evolution. Likewise, it is observed that, as the temperature of the heat transfer fluid rises, the generation of thermal energy decreases. The prices of solar thermal energy would improve the conditions offered by any conventional fuel (natural gas, diesel and fuel oil), unlike what happened just 2 years ago with natural gas. The lowest thermal power generation costs would be 3.41c€/kWht for LFC technology, and 3.69c€/kWht for PTC technology, both in Granada; being much lower than current prices (21 November 2022) for conventional fuels: 10.53c€/kWht for diesel (5.48c€/kWht, in 2021); 6.08c€/kWht for fuel oil (3.70c€/kWht, in 2021); and 7.29c€/kWht (Band I3) and 7.71c€/kWht (Band I4) for natural gas (2.35c€/kWht for Band I3 and 1.99c€/kWht for Band I4 in 2021).

1. Introduction

1.1. Background

The health, economic, and social crisis triggered by the severe acute respiratory (SARS-CoV-2) pandemic, and more recently, the conflict in Ukraine, has led to unprecedented volatility in the global energy markets.

Worldwide consumption of **fossil fuels** accounted for 82 % of primary energy usage in 2021, down from 83 % in 2019 and 85 % in 2017. Despite a reduction in the growth of **CO_2 emissions, globally,** in 2019 (with a growth rate of 0.15 %), not to mention a 2.2 % increase in 2018, and, of course, without referring to the 5.9 % decline in 2020 due to the health crisis (reaching 2011 levels, 2 Gt of CO_2, marking the largest decrease since World War II in 1945), a growth of 5.7 % occurred in 2021, reaching 33.9 GtCO_2, a value very close to 2010 levels [1]. Therefore, we are far from achieving the net-zero energy goal of 2050

* Corresponding autor.
E-mail addresses: rubenrodriguez@usal.es (R. Rodríguez Rodrigo), ricadima@ceu.es (R. Díaz Martín), mbaranda@ucm.es (M. Baranda Fernández), zjarg@usal.es (J.Á. Román Gallego), carlosmayodelrio@gmail.com (C. Mayo del Río).

https://doi.org/10.1016/j.solener.2024.112420
Received 18 October 2023; Received in revised form 22 January 2024; Accepted 17 February 2024
Available online 8 March 2024

Nomenclature

Symbols

%U	percentage of use of the available thermal energy (%)
C_I	investment cost (€)
C_{OMS}	operating, maintenance and substitution cost (€)
C_{TEU}	thermal energy unit cost, or unit cost of usable solar thermal energy (W/m^2)
C_{UL}	useful life cost (€)
d_a	aperture width of collectors (m)
d_f	distance between collector rows (m)
DNI	direct normal irradiance (W/m^2)
E_{cf}	thermal energy captured in the collector field (W/m^2)
$E_{incident\ solar}$	energy due to solar radiation (W)
E_{IPA}	available energy for industrial processes (W/m^2)
E_{output}	energy at the collector field output (Wh)
E_t	captured thermal energy in the collector field at hourly resolution (W/m^2)
E_{UIP}	usable thermal energy in the industrial process (W/m^2)
$F_{cleanliness}$	factor based on the degree of cleanliness of the collector field (%)
$F_{shading}$	factor due to shading (%)
I_t	incident solar irradiance, in hourly resolution (W/m^2)
K or IAM	incidence angle modifier
N	useful life (20 years)
$P_{abs(cond,\ conv)}$	absorber losses by conduction and convection
$P_{abs(rad)}$	absorber losses by radiation
$P_{amb(conv)}$	convection thermal losses to the environment
$P_{amb(rad)}$	radiation thermal losses to the environment
S_c	reflective surface (aperture area) (m^2)
T_{amb}	ambient temperature (K)
T_{HTF}	heat transfer fluid temperature (°C)
T_i	input temperature (K)
T_m	temperature of the fluid in the collector (K)
T_s	output temperature (K)
ω	parabolic trough collector tracking angle (°)

Greek symbols

I_{dn}	direct normal radiation (W/m^2)
I_{dni}	incident direct normal radiation (W/m^2)
c_1	first-order (linear) thermal loss coefficient (W/m^2K)
c_2	second order (quadratic) thermal loss coefficient (W/m^2K^2)
η_0	optical efficiency or maximum collector efficiency **(%)**
α	absorbance (%)
γ	interception factor (%)
Δ_t	time interval (h)
ΔT	thermal jump ($T_m - T_{amb}$) (K)
η_{cf}	instantaneous efficiency in the collector field (%)
η_{cond}	conduits efficiency (primary and secondary circuit pipes (%)
η_{ehe}	external heat exchanger efficiency (%)
η_{global}	global efficiency (%)
$\eta_{ópt\ (0°)}$	peak optical efficiency (%)
η_t	thermal efficiency (%)
η_{tank}	tank efficiency (%)
θ	incidence angle (°)
θ_{long}	longitudinal incidence angle (°)
θ_{long}	longitudinal incidence angle (°)
θ_{trans}	transversal incidence angle (°)
θ_{trans}	transversal incidence angle (°)
ρ	reflectivity mirrors (reflectance)
τ	transmittance (%)
η	instantaneous efficiency or yield (%)

Subscripts

i	initial instant
f	final instant

Acronym

CIP cleaning	Clean In Place cleaning
CPC	Evacuated tube with compound parabolic concentrator
CPI	Consumer price index
CSP	Concentrated solar power
ESTIF	European Solar Thermal Industry Federation
HTST	High-Temperature Short-Time Pasteurization
IEA	International Energy Agency
IRENA	International Renewable Energy Agency
LCA	Life Cycle Analysis
LCUTE	Levelized unit Cost of the Useful Thermal Energy
LFC	Linear Fresnel Collector
NZES	Net Zero Emissions Scenario
OPEC	Organisation of Petroleum Exporting Countries
PTC	Parabolic Trough Collector
SDS	Sustainable development scenario
SHIP	Solar Heat for Industrial Processes
STAGE-STE	Scientific and Technological Alliance for Guaranteeing the European Excellence in Concentrating Solar Thermal Energy
TMY	Typical Meteorological Year
UHT	Ultra-High Temperature processing, Ultra-Heat Treatmente, or Ultra-pasteurization
VAT	Value Added Tax

(as outlined in the Paris Agreement[1] 2015 or the Sustainable Development Goal).

Primary energy demand increased by 5.52 % in 2021, exceeding 2019 levels by 1.31 % (in 2020, it fell by 3.99 %). The reason for the drop in 2020 was attributed to the health crisis; however, the slowdown in 2019 was due to slower global economic growth and milder weather that affected the energy consumed for heating and cooling (it is estimated that the weather caused a reduction in energy consumption of 0.8 % [2]) (Fig. 1).

In 2021, the **industrial sector** was responsible for the emissions of 9.4 Gt of CO_2, reaching pre-pandemic levels, assuming a growth of 3 %. They accounted for a quarter of global emissions (not including emissions resulting from the electricity consumption which is used in the industrial processes). In the net zero emission scenario for 2050, industrial emissions must be reduced to 7 Gt of CO_2 by 2030 [3], and to do so, emissions should be reduced by almost a quarter of actual emissions, which is approximately 3 % per year, requiring accelerated political action (Fig. 2).

Fossil fuels continue to be a dominant energy source in the industrial sector, and their use continues to grow. If the targets of the net-zero scenario are to be met, the demand for fossil fuels must be curbed, thereby necessitating an increase in the use of renewable energy and the adoption of energy efficient strategies. In 2020, several international

[1] The Paris Agreement is a legally binding international treaty on climate change. It was adopted by 196 parties at COP21 in Paris on 12 December 2015 and entered into force on 4 November 2016. It aims to limit global warming to well below 2°C, preferably to 1.5°C, compared to pre-industrial levels. https://unfccc.int/es/ [accessed 08 August 2021].

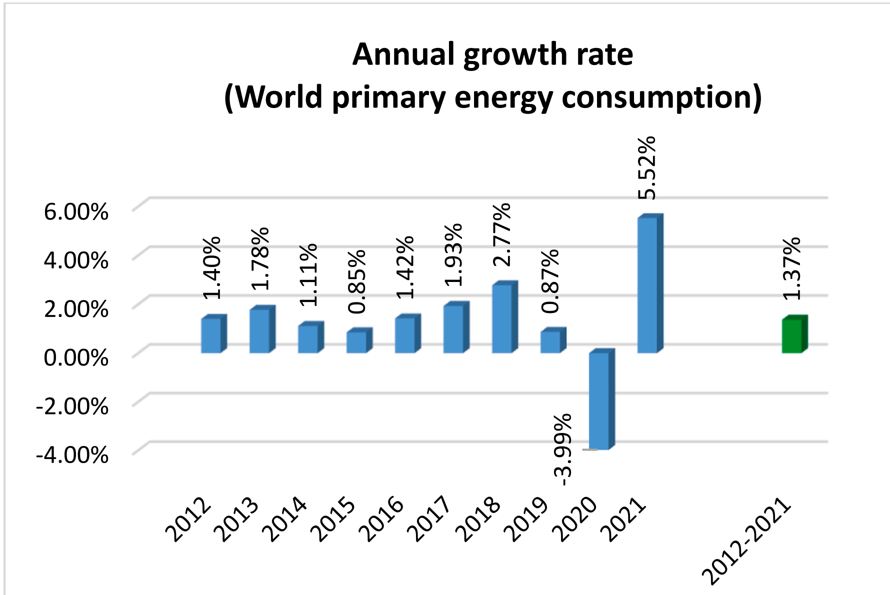

Fig. 1. Annual growth rate corresponding to the increase in world primary energy consumption 2001–2020.

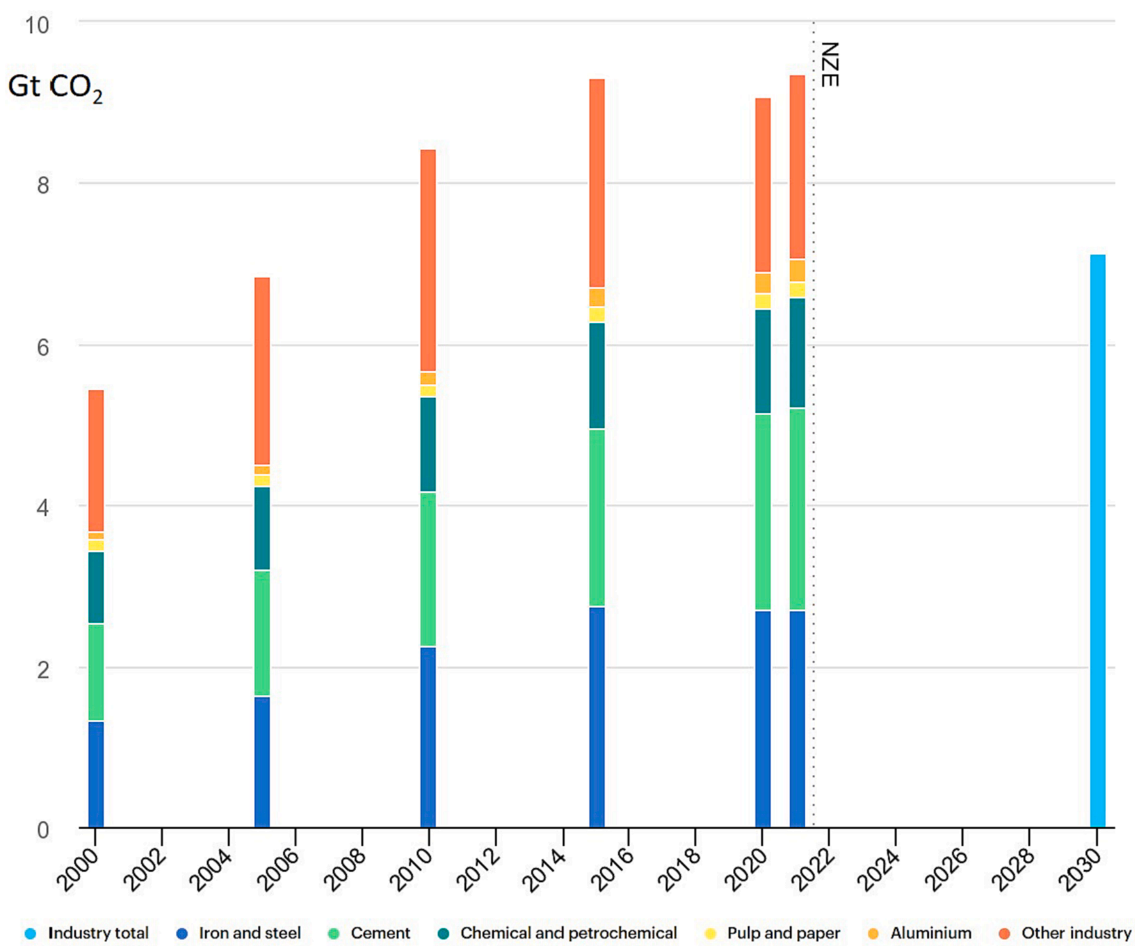

Fig. 2. Direct CO_2 emissions from industry in the net zero scenario (2000–2030) [4].

organisations published a joint report highlighting the importance of decarbonising industrial heat demand [5].

Despite these challenges, SHIP systems have not experienced their best moments. Not only do potential customers desire short payback periods, but also few plants present this alternative as an opportunity. Additionally, the extended development time of projects poses significant obstacles. This is compounded by current energy prices, leading companies to focus their investments on photovoltaic technology because of their higher profitability from installation.

In 2021, 71 new systems (36 MWt) were commissioned, compared to 85 (93 MWt) in 2020 and 86 (251 MWt) in 2019 [6]. Notably, China reported only seven new systems in 2021, down from 30 in 2020 (global leader). This decline is attributed to the stringent closures in the first quarter of 2022, preventing employees from collecting data, as China represents the largest market in the sector. The number of new SHIP systems outside China increased from 55 (22 MWt) in 2020 to 64 (27 MWt) in 2021.

The preceding data can be enhanced by confirming the technical (energy) and economic viabilities of Process Heat Generation Systems (*SHIP systems*). This confirmation would propel the implementation of medium-temperature solar concentration technologies in the agri-food industry, with the dairy industry being the sector with the highest demand globally, thereby promoting its development and improvement.

1.2. Literature review

Several studies have looked into the technical and economic performance of different systems, in January 2017. **The solar heating potential of industrial processes in the Indian dairy sector and the corresponding mitigation of carbon emissions** from them were analysed by studying the effect of varying direct normal irradiation (different plant locations) on the annual performance of solar heating systems; however, only two technologies namely the parabolic dish and parabolic trough, were studied [7]. Shortly thereafter, in November 2017, a study on the **optimisation of a multi-temperature solar heating system (four processes with different temperature levels and load profiles)** was conducted for a **milk processing plant in Casablanca**, where the use of solar energy to meet part of the heat demand was discussed as an economic opportunity for developing countries such as Morocco; however, only the evacuated tube technology was considered [8].

In June 2018, **the financial viability of solar heating for industrial processes and the cost of carbon mitigation in a dairy industry in India** were analysed; however, only parabolic trough technology was considered. *Seven locations* with dairy sector plants were studied to estimate the annual production of useful thermal energy. It was concluded that, *in LCUTE thermals, it did not seem viable, with the payback period being very high* [9], in contrast to the conclusions drawn in this study.

In April 2021, **an energy efficiency study conducted in the Dutch dairy sector** on energy use in plants found that *the use of solar panels was the most significant determinant for reducing fossil fuel consumption and that the increase in energy efficiency sought by government policies is counteracted by the trend towards mechanisation* (automatic milking systems lead to lower energy efficiency), *and that* increasing the *economies of scale in milk production helps to improve energy efficiency per unit* [10].

All of the above refer specifically to the dairy sector; however, there are other studies, such as the one conducted in December 2020 on the **integration of solar heat in the lead extraction process**, using **flat plate and evacuated tube collectors** for **7 different mining countries in the world**, concluding that *the most efficient system would be based on evacuated tube collectors* with solar loop heat exchangers [11]. Another more generic study, in January 2020, dealt with **environmental-economic optimisation in the implementation of parabolic trough collectors in low and medium enthalpy industrial process heat generation in Mexico**. It was concluded that *diesel was the most cost-effective support fuel and natural gas the least viable* [12].

As can be seen, different studies exist; however, they deal with specific cases: the energy demand in the dairy sector in India; a single technology (evacuated tube collector) in Morocco; the installation of metering equipment in a flat plate plant with a single fuel (fuel oil) in Taiwan; obtaining useful thermal energy and its unit cost with a single technology (parabolic trough) in India; two fuels, different climate zones, and solar field surfaces, but with a single technology (parabolic trough); and the calculation of useful thermal energy in seven countries, but only for flat plate and evacuated tube collectors. In other words, none include all the information that will be provided in this manuscript.

1.3. Scope and contribution

As has been discussed, **there are no detailed studies** that analyse the technical-energy and economic aspects of the integration of the two most representative medium-temperature concentrating solar power technologies currently used for SHIP systems in the dairy sector namely the *linear Fresnel collector (LFC) and parabolic trough collector (PTC)*, considering that there are no plants in this sector that integrate these systems in Spain where the three most commonly used conventional fuels are natural gas, diesel and fuel oil, and with the current energy costs after the volatility in the markets that has been generated after the pandemic and the conflict in Ukraine. The most widely used solar technologies are the flat plate (FP), compound parabolic concentrator (CPC), linear Fresnel collector (LFC), and parabolic trough collector (PTC). The FP and CPC technologies operate in lower temperature range. LFC and PTC technologies best align with the temperature ranges required for industrial dairy processes.

The **novel contribution of this work** is that it provides a systematic analysis to assess the potential of SHIP system integration in the dairy sector (the food subsector with the highest number of SHIP systems installed worldwide). To the best of our knowledge, this is the first time such an extensive study has been carried out, that has gathered data on the energy consumption of several plants distributed across different geographical locations in Spain confirming confirming the economic viability of integrating this type of SHIP systems. This is in contrast to the conclusions drawn by other studies seeking to promote innovative technologies aimed at improving the efficiency of industrial processes in the dairy sector.

Of all the companies in the dairy sector that agreed to provide the requested data, two plants were selected based on size, sufficient to consider a representative sample (This is important because the surface area of the solar field produces economies of scale, reducing investment costs as the surface area increases), with the aim of carrying out a comparative study of the energy and cost savings that could be achieved depending on the type of concentrating solar power technology and several other variables. For this purpose, a series of hypotheses were established: availability of surface area for the installation of the solar field, the percentage of thermal energy utilization (decisive in determining the cost of thermal energy generation), the required thermal level (common to all companies in the dairy sector), as well as assumptions that have allowed the assessment of the potential for thermal energy production in Spain for different geographical locations based on existing climatic zones (according to the Technical Building Code, (CSIC, 2022)). These hypotheses, along with the considered variables, are described in section 3, 'Methodology.

Subsequently, we analysed which technology would be the most appropriate, using simulation tools and by carrying out different calculations based on similar SHIP system integration conditions (because the efficiency varies depending on the integration point), over a time horizon of 20 years and for three different scenarios based on the evolution of prices of conventional energy sources (medium, bullish, and very bullish, representing only the results obtained for the most unfavourable scenario which was the medium).

Likewise, the cost of solar thermal energy available to the industrial process was determined for the different temperature levels required in the dairy sector processes (120, 140, 160, 200, 240 and 280 °C), comparing it with conventional energy sources, to finally obtain the annual net benefit, in relation to the investment cost of the installation and considering its useful life (20 years), in all the locations studied, and for the three scenarios considered.

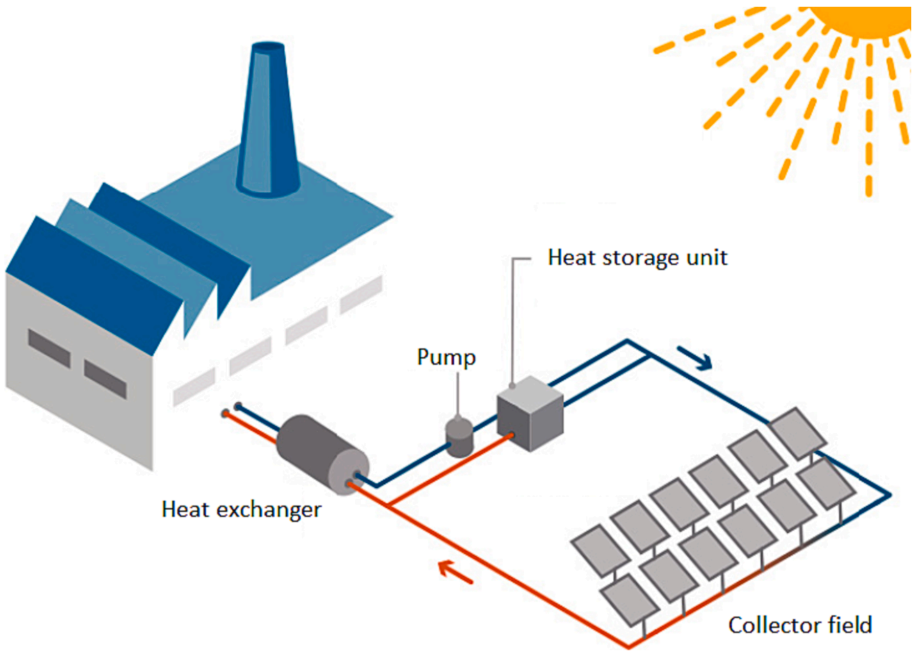

Fig. 3. Solar heat for industrial processes [14].

Table 1
Classification criteria for SHIP Systems.

Criterion	Options
Heat transfer fluid	Vapour
	Liquid (water, thermal oil)
	Air
Collector circuit	With recirculation
	Without recirculation
Heating system	Direct
	Indirect
Auxiliary system	Without auxiliary system
	Series
	Parallel
Storage	With accumulation
	Without accumulation

2. System description

2.1. Principles of the SHIP systems

A SHIP system incorporates a heat storage unit, thereby increasing the period of the day in which heat is supplied by compensating for the variations in solar resources. A system is considered very large or large-scale when it has more than 350 kWt or has more than 500 m^2 of glazed and concentrated collectors [13]. (Fig. 3).

SHIP systems possess two fundamental characteristics: their size, which is determined by the energy consumed, and the requirement for integration with the conventional energy system used in the process. These systems can be classified based on the following criteria: (Table 1)

There are many different configurations of SHIP systems. The most significant configuration is based on the heat-transfer fluid. In the case under study, the system consists of a liquid that is recirculated, an indirect system (external heat exchanger) and an auxiliary system in series; it is powered by conventional energy and has storage.

2.2. Integration

Given its high potential, the integration of solar heat into industrial processes has increased with the aim of boosting the implementation of this technology in the market. Tools have been developed to familiarise managers and energy consultants with solar heat for industrial processes by enabling them to assess the feasibility of integrating a SHIP system into a given plant, including the estimating of size and performance, storage, and solar field dimensions, as was the case with the German project SolFook Solar Heat for the Food Industry in 2016 [15].

The processes within a plant must be studied well to determine the viability of integrating a SHIP system and to identify and locate heat dissipation points through a pinch analysis, which estimates the maximum heat recovery potential before integrating solar heat technology. For example, considering that the focus of this study is on the dairy sector, once it has been decided to integrate a SHIP system it must be noted that pasteurisation takes place at different temperatures depending on the method used HTST (72 °C for 15 s) or UHT (138 °C for 2 s, which implies a lower degradation of the food by minimising the exposure period), so the type of technology used must be analysed, as high temperatures are needed in the production of steam to reach these temperatures, (unless, once the installation has been analysed, it is found that this increase in temperature is more profitable, but not sustainable, if it is achieved by means of an auxiliary boiler). Therefore, the present study considers medium temperature systems (between 150 and 400 °C, although different sources consider the range for medium temperature to be between 100 and 250 °C).

The SHIP system can be integrated at different points during the installation. We can preheat the makeup water, heat transfer fluid, or the industrial process directly, or even combine different options.

In the Integration Guide [16] (initially intended for processes requiring temperatures up to 100 °C, but equally valid for medium temperatures), different integration approaches are shown for two clearly differentiated levels: **supply** and **process**. **The first level** allows for a much more universal integration and higher temperatures and is more flexible as the generation system is less dependent on possible changes in the process. However, the best option depends on the industry involved.

2.3. Types of collectors to consider

The aim of this study is not to develop new technologies, but to integrate some of them into an industrial process in the dairy sector; therefore, **two existing commercially developed concentrating solar**

Table 2
Most frequent energy uses in the dairy sector.

ENERGY	MOST FREQUENT USES	EQUIPMENT
Thermal	Steam and hot water generation, cleaning.	Pasteurisation, sterilisers, drying and cleaning systems.
Electrical	Cooling, ventilation, lighting, operation of equipment	Pumps, agitators, lighting, etc.

power technologies are considered for the purpose of this study, namely: *LFC and PTC.*

To determine the efficiency of the collectors that allows a uniform comparison of the results, a method independent of the available solar technologies is required, which is developed as per the ISO 9806:2020 standard [17] and comprises two models: steady-state and quasi-dynamic (used in concentrating collectors). The optical and thermal characterisation parameters obtained according to the criteria of this standard are available in the Solar Keymark database [18] (certification mark for solar collectors, promoted by ESTIF, the European Solar Thermal Industry Federation, which is responsible for confirming that a product complies with European standards and norms), which, combined with climatic data and operating conditions, allows for the determination of the instantaneous power of the collector and, consequently, the collector's thermal energy production during a specific period and under specific operating conditions. In addition to ISO 9806:2020, there are other standards for solar collectors, such as ASTM E 905–87 which is applicable to solar-tracked collectors, and ASHRAE 93–2003 which is applicable to non-tracked collectors [19].

Suppliers have different collector models whose technical parameters such as materials, designs, certifications, and geometric, optical, and thermal information are continuously evolving. To keep this information updated, an online database for concentrating solar collectors was created so that manufacturers could enter what they considered appropriate. This would later be reviewed and made available to the public. This database corresponds to the STAGE-STE project [20] (as opposed to the Solar Keymark collector database used for "flat plate" and "evacuated tube" collectors). Most of the collectors are of the parabolic trough type and that adopting the linear Fresnel technology; hardly any of the manufacturers of other types of collectors have entered their data.

2.4. A study of the dairy sector

Energy in the dairy industry is used to supply energy to the equipment for different processes, such as heating, evaporation and drying, pasteurisation, cooling and refrigeration, compressed air generation, and lighting. This study focuses on the generation of process heat, and therefore, on all processes that use the steam produced in boilers (Table 2).

Approximately 80 % of the requirements of this type of industry are met by steam generation through the combustion of fossil fuels. The remaining 20 % is supplied with electrical energy (refrigeration, lighting, electric motors, etc.). These percentages were confirmed during the fieldwork.

Operations with a higher consumption of thermal energy, such as pasteurisation/sterilisation of milk and CIP cleaning (automatic washing systems that do not require the dismantling of production equipment, which consists of recirculating the cleaning solution through the components of the process line, such as pipes, heat exchangers, pumps, and valves), account for up to 80 % of the total thermal energy consumption of the plant.

3. Methodology

Different tools were investigated to obtain the useful energy output at the collector field (TRNSYS v.18.03.0002 [21], COLSIM 0.63 [22], INSEL 8.2 [23], T*SOL 2018 [24], GREENIUS 4.5.0 [25], SAM [26], TRANSOL [27], and IPSEPRO [28]), and the one that adapted best to the objectives of this study (Polysun 12.0 [29]) was selected. The most common SHIP system for this type of installation having the following features was chosen:

- Heat transfer fluid: water or thermal oil.
- Indirect heating system, through an external heat exchanger.
- Auxiliary system in series, fed with conventional energy.
- Storage: with storage.

The solar heat concentrating system provides part of the energy required by the industrial process through the heat exchanger (primary circuit) which is a collector field external heat exchanger, where the solar radiation incident on the collector field is used to increase the thermal energy of the heat transfer fluid used). The heat transfer fluid is stored in the storage tank, from where the hot water would be collected so that the auxiliary boiler connected in series and powered by conventional fuel (natural gas, diesel, or fuel oil), raises its temperature to generate the steam, at a given pressure and temperature, required for the industrial process. The schematic of the configuration is as follows (Fig. 4):

For this purpose, the following variables and hypotheses are considered:

- Variables:

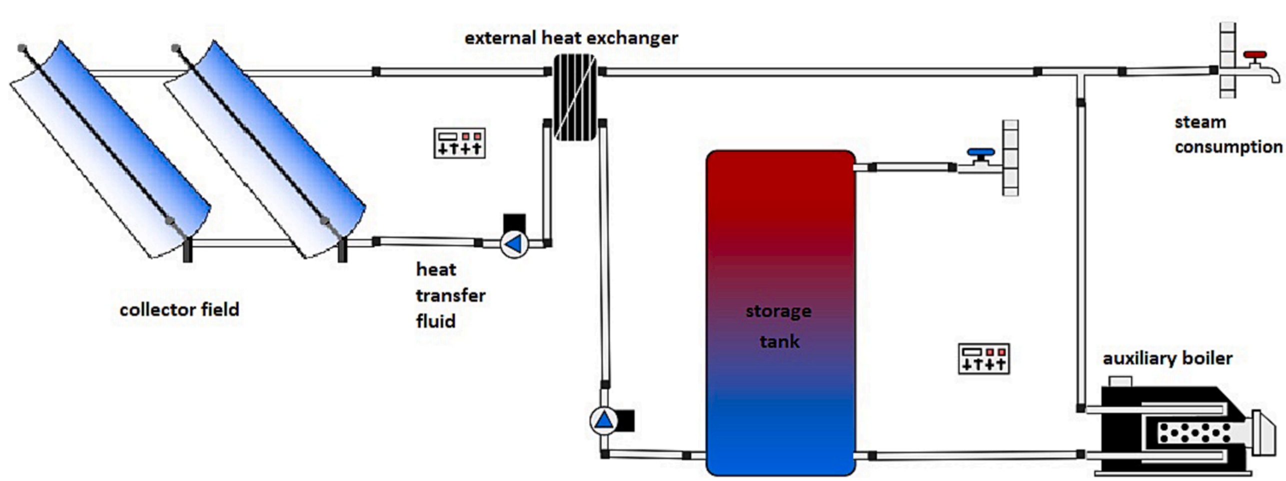

Fig. 4. Diagram of the configuration considered (Polysun 12.0) [29].

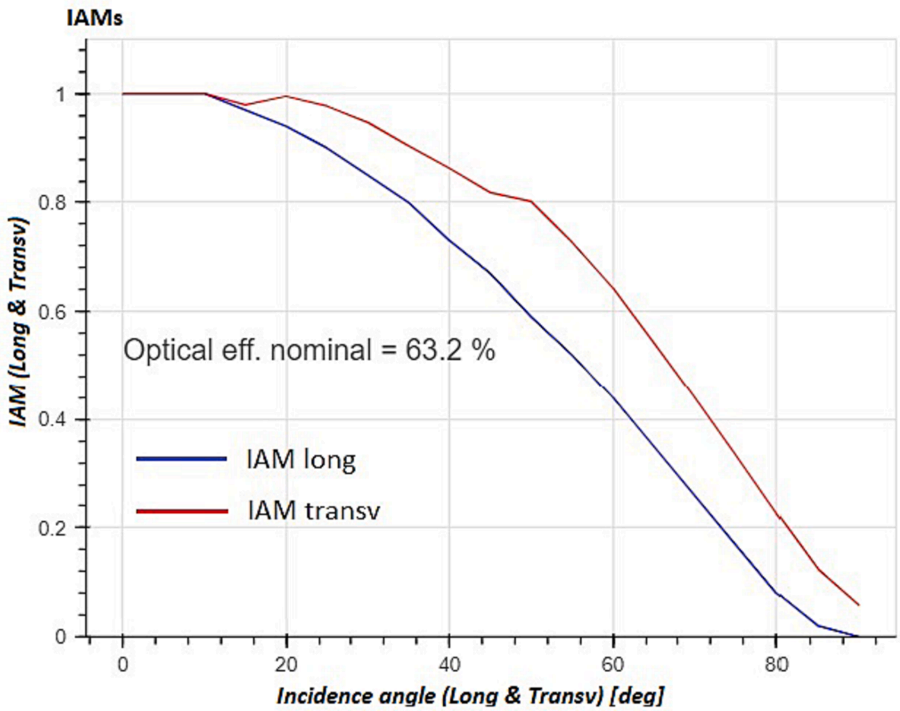

Fig. 5. Incidence angle modifier for linear Fresnel collectors - Solatom FLT20 [31].

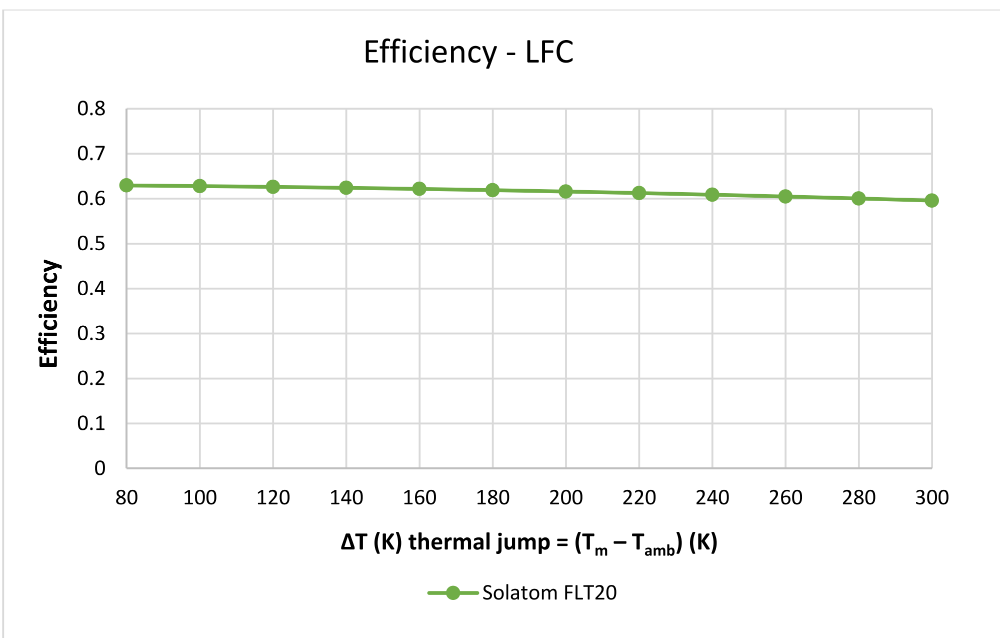

Fig. 6. Efficiency curve. LFC Technology - Solatom FLT20 Linear Fresnel Collector.

- Locations: Eight climatic zones with different solar resources were used to observe the differences that would occur in the generation of thermal energy in the collector field of each of them. Increasing the radiation increased the installation performance.
- These two plant sizes are representative of the dairy sector in Spain (annual demands of 10 and 60 GWh).
- Technology: LFC and PTC.
- Fuel: natural gas, diesel and fuel oil.

• **Hypotheses:**

- The steam demand is higher than the steam production, considering the constant demand profile of the three detected during the data collection stage. Percentages of available thermal energy used (%U): 70 % and 100 %.
- Industrial process using a single thermal level, studying different set point temperatures 120, 140, 160, 200, 240 and 280 °C, and representing results for 200 °C.
- No heat recovery from other processes.

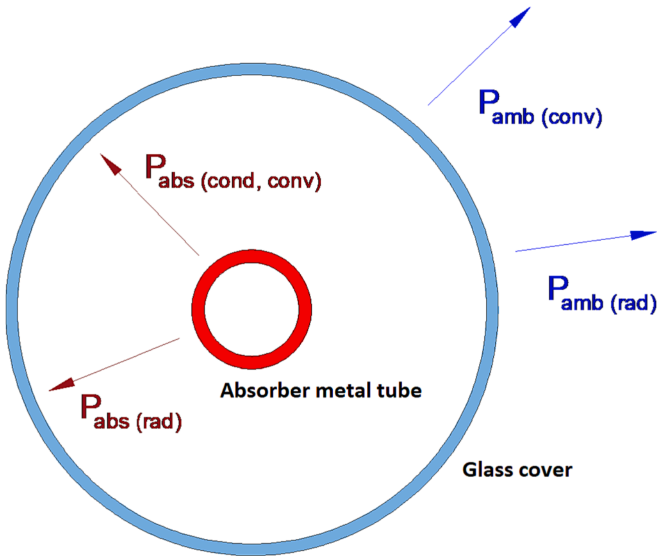

Fig. 7. Thermal losses in PTC.

- Solar fraction: There are no space limitations for the installation of the SHIP system, analysing two cases where the values reach 15 % and 30 %.
- The cleanliness of the collector field was not considered as a variable, and a predetermined average value was established.
- Energy losses in the distribution system, exchanger and storage.
- Operation, maintenance and replacement costs.
- The initial investment does not require prior financing.

To define the solar fraction, the amount of heat required for industrial processes was assessed by determining the amount of heat that could be effectively supplied. The required temperature was considered along with the costs associated with the implementation and operation of the solar power system. The average available surface area for deploying the SHIP system in the 17 analysed plants was also considered. This surface area corresponded to values of the solar fraction ranging from 15 % to 30 %. Furthermore, solar fractions of 15 % and 30 % would ensure the full utilisation of energy with minimal losses. Designing for higher solar fractions would lead to generation peaks at specific times of the day that could not be harnessed owing to the demand profiles of the dairy sector. This would increase the period for which the energy would have to remain in the storage system, causing suboptimal system performance.

Because the auxiliary boilers, piping, heat exchangers, and storage systems, which are common elements in a SHIP system, have different sizes and diameters, they are not included in the study, and the focus is exclusively on the collector field. These elements will be included in future research because they require specific designs for each plant or industrial process.

3.1. Efficiency characterization of the different technologies

3.1.1. Linear Fresnel collector (LFC)

The performance equation or instantaneous efficiency characteristic of this type of technology is as follows [30]:

$$\eta = \eta_0 - c_1 \cdot \frac{\Delta T}{I_{dni}(\theta)} - c_2 \cdot \frac{\Delta T^2}{I_{dni}(\theta)} \quad (1)$$

where:

$$I_{dni} = I_{dn} \cdot \cos(\theta) \quad (2)$$

The selected collector is the **FLT20** model from **SOLATOM**. The collector is supplied as 6-metre modules, and is configured according to the requirements of the industrial process. The technical characteristics and the incidence angle modifier are detailed on its website (Fig. 5) [31]:

The efficiency curve of the Solatom FLT20 collector is shown below (Fig. 6), for which the following values are considered:

- $T_{amb} = 20$ °C; DNI = 1000 W/m^2; $\eta_0 = 0.632$; $c_1 = 0.001$ W/m^2·K; $c_2 = 0.0004$ W/m^2·K^2.

3.1.2. Parabolic trough collector (PTC)

For this type of technology, the efficiency will not be characterised in the same way as in the previous case (instantaneous value); rather, the energy balance will be used by considering the transformation of solar radiation into thermal energy as a series of processes that involve losses or associated yields. These losses are classified into three types: geometric, optical, and thermal [32].

a) *Geometric losses*

The geometry of this technology implies a decrease in the effective capture area. The losses can be classified into two categories.

- *Losses due to shadows:* these are due to the relative position of the collectors as they cast shadows on the closest collectors. These losses are minimised by increasing the distance between the rows.
- *Losses due to the tracking system:* Normally, this type of technology has tracking on a single axis, with the *incidence angle* (θ) causing a loss of useful reflective surface at its ends. When this angle is different from zero, the effective capture area is reduced; in addition, other parameters such as transmittance, absorptance, and reflectance are altered, and their values are maximum when the incidence angle is zero. The *incidence angle modifier* (K) quantifies the influence of the incidence angle on the collector efficiency.

b) *Optical losses*

These are caused by anomalies in the system components (absorber, glass tube, reflecting surface, etc.), which means that not all incident direct solar radiation reaches the heat-transfer fluid circulating inside the absorber tube.

The four parameters that affect the optical losses when this type of technology is utilised are:

- *Transmittance* (τ) of the glass cover that contains the metallic absorber tube both to protect it and to reduce thermal losses. The ratio of the radiation passing through the glass cover to the total incident radiation is typically between 90 and 95 % (depending on whether an antireflection treatment has been applied to the glass).
- *Absorbance* (α) of the selective surface of the absorber tube. This represents the amount of incident radiation that is absorbed (between 90 and 96 %).
- *Reflectance* (ρ) of the reflector surface whose typical values are close to 90 % (not all incident radiation is reflected). In fact, at the Plataforma Solar de Almería, the reflectance value with good cleaning reached 92 %, decreasing by 0.26 % per day owing to progressive soiling.
- *Interception factor* (γ) which is the amount of solar radiation reflected from the collector surface that does not reach the glass cover of the absorber tube. This may be due to imperfections in the mirrors, positioning of the collector, etc. Its characteristic value is typically 95 %.

Having defined the four parameters, the peak optical efficiency of the PTC technology is obtained:

$$\eta_{ópt(0^\circ)} = \tau \cdot \alpha \cdot \rho \cdot \gamma \quad (3)$$

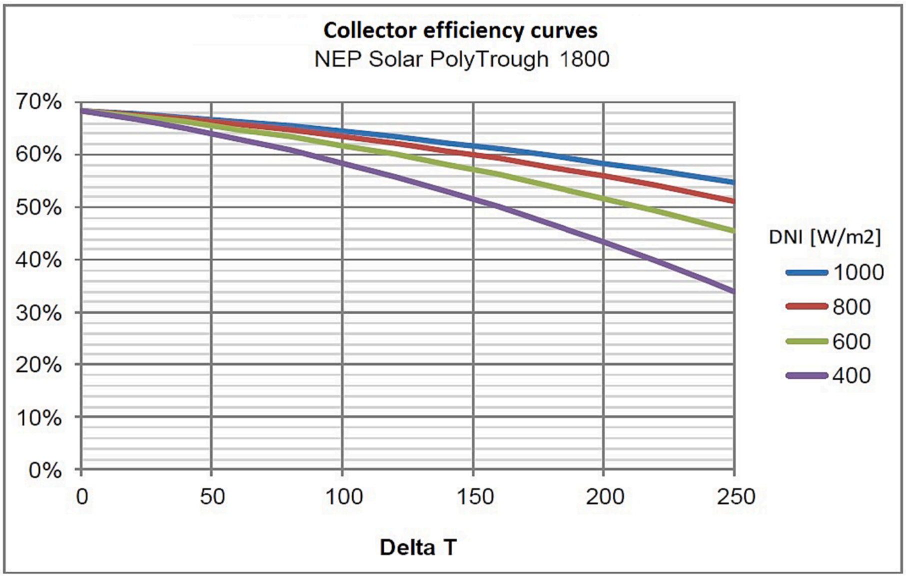

Fig. 8. Efficiency curves of the parabolic trough collector NEP Solar PolyTrough 1800 [33].

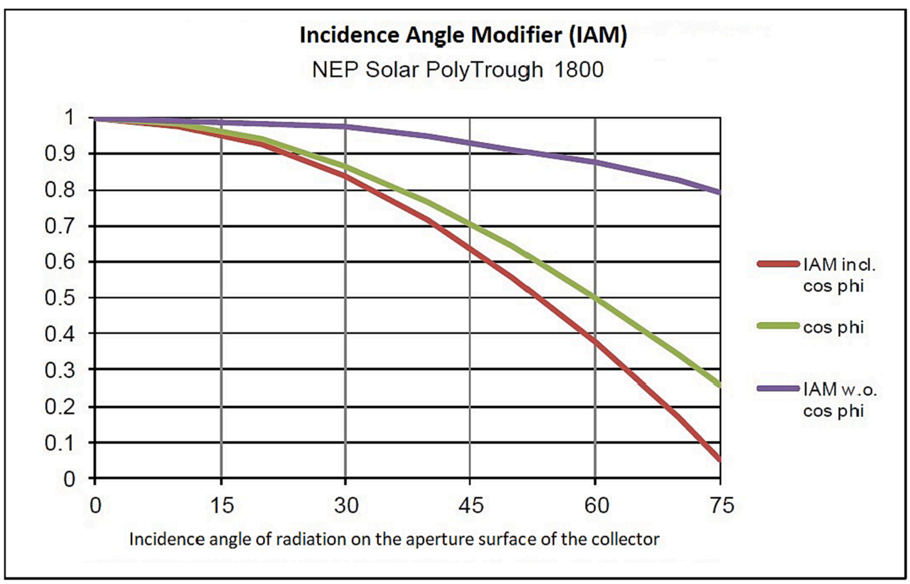

Fig. 9. Incidence angle modifier (IAM) for the parabolic trough collector. NEP Solar PolyTrough 1800 [33]. Note: These diagrams show the results of the numerical simulations and are not based on experimental data.

c) *Thermal losses*

In this type of technology, these losses are somewhat less significant than the optical losses and are produced in the absorber tube (the most significant) and in the pipes through which the heat-transfer fluid flows. Losses associated with the absorber tube would be the result as a result of

- conduction through the supports of the absorber tubes.
- radiation, convection and conduction from the absorber tube to the glass cover.
- convection and radiation from the glass cover to the environment.

It is important to note that there is a vacuum between the absorber tube and glass cover; therefore, the losses due to conduction and convection from the absorber tube to the glass cover are neglected (only the losses by infrared radiation would remain).

The overall thermal losses are quantified using equations based on the experimental results instead of using the equations defining each of the heat transfer processes mentioned (Fig. 7).

Once the types of losses are specified, the collector efficiency is defined. Three different efficiencies and representative parameters were determined.

- *Optical efficiency*: or the incidence angle of 0° [peak optical efficiency, $\eta_{ópt\ (0^\circ)}$], expressed according to Equation (5).
- *Thermal efficiency (ηt):* where thermal losses are taken into account.
- *Global efficiency (ηglobal):* considering all losses (geometrical, optical and thermal).
- *Incidence angle modifier (K):* determines the optical and geometric losses for angles of incidence other than zero, that is, those that are not considered for the $\eta_{ópt(0^\circ)}$, as they would be:
- Geometric losses at the collector end.

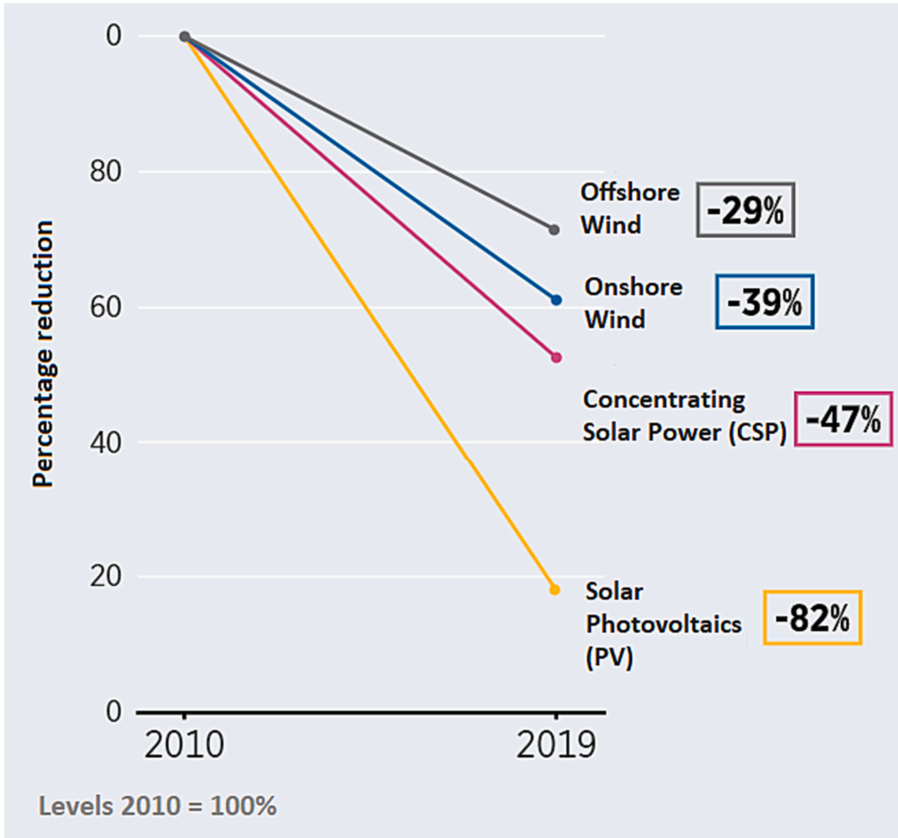

Fig. 10. Cost reduction in renewable energy, per kWh generated since 2010, [34].

- Blocking of concentrated radiation by the receiver tube supports (absorber)
- Influence of incidence angle on absorptance and transmittance of the absorber tube and reflectance of the collector surface (mirrors).

Therefore, the energy at the output of the collector field can be determined as follows:

$$E_{output} = E_{incident\ solar} \cdot F_{shading} \cdot F_{cleaning} \cdot \eta_{\acute{o}pt(0^{\circ})} \cdot \eta_t \cdot K \cdot \Delta t \quad (4)$$

Siendo:

$$E_{incident\ solar} = S_c \cdot I_{dn} \cdot cos\theta \quad (5)$$

$$\mathrm{F}_{\mathrm{shading}} = \frac{d_f}{d_a}\left|\sin\left(\frac{\pi}{2} - \omega_s\right)\right| \quad (6)$$

$$K = (1 - 2.23073 \cdot 10^{-4} \cdot \vartheta - 1.1 \cdot 10^{-4} \cdot \vartheta^2 + 3.18596 \cdot 10^{-6} \cdot \vartheta^3 - 4.8509 \cdot 10^{-8} \cdot \vartheta^4) \quad (7)$$

For the case under study the following values will be considered:

- $\tau = 0.95$ (°/1); $\alpha = 0.95$ (°/1); $\rho = 0.92$ (°/1); $\gamma = 0.95$ (°/1); $\eta_t = 0.93$.
- Tracking system: North - South.

In the selection of the collector with **parabolic trough technology**, after carrying out the same analysis as for the previous technology (network information and Polysun 12.0 program database), it was decided to use the PolyTrough 1800 model from NEP Solar in the simulations. Its characteristics are described on their website (Figs. 8,9) [33]:

3.2. Economic analysis

3.2.1. Cost of concentrating solar technologies

The highly competitive market has contributed to lower installation costs and, therefore, a shorter payback time.

According to the latest estimates by IRENA, the cost of photovoltaic technology is much lower than it was ten years ago; however, this is not the case with solar thermal technology for which the reduction in cost has been to the same extent (Fig. 10):

Therefore, there is a clear decrease in electricity generation costs, which can be extrapolated to medium-temperature concentrating solar power systems for thermal power generation as they share PTC and LFC technologies.

As this is a long-term investment, not only the payback period of the investment but also the economic flows that remain in the form of savings once the investment has been recovered are important. Therefore, the operation, maintenance, and replacement costs are important.

Thus, a favourable evolution of the cost of this type of technology in the market has been noted, but its magnitude has not been quantified. This is a complex task because this type of information is not usually available, and the bibliographical references that speak of it are usually not up-to-date. This difficulty is multiplied not only when it is necessary to quantify the costs of operation, maintenance, and replacement, but also when it is necessary to define the economy of the scale factor that manifests itself when increasing the size of the collector field.

a) *Parabolic trough technology (PTC)*

In the SHIP system database [35], the following systems were located for which the turnkey price per m^2 of the gross PTC collector area was determined (including solar collectors, piping, support construction, storage, design, and commissioning, excluding VAT). We created two

Table 3
Investment cost for SHIP systems with PTC technology in the dairy sector.

Project	La Trinidad	Lácteos Mojica	Quesera Lácteos Ticoy, S.A. de C.V.	Lechera Guadalajara SELLO ROJO	Centro Lechero Cooperativo de los Altos SCL	Cremo SA	Emmi Dairy Saignelégier	Lesa Dairy
Company	Inventive Power	Inventive Power	Inventive Power	Inventive Power	Inventive Power	NEP Solar AG	NEP Solar AG	NEP Solar AG
Year	2017	2016	2015	2015	2015	2013	2011	2010
Collector model	Power Trough 110	Power Trough 110	Power Trough 110	Power Trough 110	Power Trough 110	PolyTrough 1800	PolyTrough 1800	PolyTrough 1200B
Gross collector area (m^2)	226.78	132	250	1641.25	422	581	627	115
Collector opening area (m^2)	120	132	99	429	197	581	627	115
Installed thermal power (kWth)	59.9	59.88	42	240	94,5	330	360	67
HTF	water	water	water	water	water	water	water/glicol	thermal oil
Storage	Steam storage tank	short-term water heating	short-term water heating	short-term water heating	short-term water heating	without storage	short-term water heating	without storage
Storage volume (litres)	4800	4500	6000	50,000	9500		15,000	
Conventional boiler	Water heating	Water heating	Water heating	steam boiler	Water heating	Hot water boiler	Hot water boiler	steam boiler
Fuel	natural gas	other	other	natural gas	natural gas	fuel oil	fuel oil	fuel oil
Process	Boiler preheating	Boiler preheating	Pasteurisation Ice cream	Pasteurisation	cleaning equipment	Boiler preheating	Steam for different dairy processes	dairy process
Operating unit		Pasteurisation	Pasteurisation	Pasteurisation	cleaning	Sterilisation (milk processing, coffee cream production).	General heating processes	General heating processes
Integration point	make-up water heating	make-up water heating	Supply line heating	Heating of the process medium (pasteurisation heat exchanger)	Supply line heating	Supply line heating	Heating of the supply heat storage.	Supply line heating
Process temperature (°C)	90	20–95	20–95	85	19–92	150 y 110		
Collector temperature (°C)	20–90			70–95		170 y 125	140—180	
Investment (€)	48,050	36,894	28,046	160,000	46,144	700,000	300,000	252,000
Subsidies	no	no	no	no	no	25 %	95 %	40 %
Cost per area (€/m^2)	**211.88**	**279.5**	**112.18**	**97.49**	**109.35**	**1204.82**	**478.47**	**2191.3**
Solar fraction (%)				40	40		15	5

Table 4
Updated prices according to the evolution indicated by IRENA (PTC technology).

Surface area Solar field (m^2)	Cost per surface area (€/m^2)	Cost per updated surface area (€/m^2)
226.78 (year 2017)	211.88	167.64
132.00 (year 2016)	279.50	206.55
250.00 (year 2015)	112.18	77.05
1641.25 (year 2015)	97.49	66.96
422.00 (year 2015)	109.35	75.10
581.00 (year 2013)	1204.82	701.69
627.00 (year 2011)	478.47	228.71
115.00 (year 2010)	2191.30	933.06

comparison tables, one per manufacturer, for the dairy sector so that the influence on the price, depending on the manufacturer, could be observed, as well as differentiating the sizes of the installations (Table 3).

The above tables show that, for the manufacturer Inventive Power (with all projects analysed in Mexico), the prices range from 97.49 €/m^2 for the largest plant (1641.25 m^2) to 279.5 €/m^2 for the smallest plant (132 m^2), clearly showing the economy of scale factor. In contrast, for NEP Solar (with Switzerland as the location of the projects analysed), there is no clear correlation, with prices varying between 478.47 €/m^2 for the largest installation (627 m^2) and 2191.3 €/m^2 for the smallest installation (115 m^2). The installations of the second manufacturer are older than those of the first; therefore, they do not reflect current costs, indicating that they have been considerably reduced. Different studies have reported the following values, including the costs associated with the complete installation of the solar power system:

- Study 1 (2010) [36]: 512 €/m^2.
- Study 2 (2011) [30]: 330 €/m^2.
- Study 3 (2014) [37]: 190–440 €/m^2.

According to IRENA [34], CSP costs decreased by 47 % from 2010 to 2019, which is equivalent to 5.22 % per year (linear); applying this trend since the year in which the previous plants were commissioned, the costs would be as shown in Table 4.

The cost of installation of studies updated according to these developments would be as follows:

- Study 1 (2010): 218.01 €/m^2.
- Study 2 (2011): 157.74 €/m^2.
- Study 3 (2014): 120.57 – 279.22 €/m^2.

Table 5
Investment cost for SHIP systems with LFC technology.

Project	Nuova Sarda Industria Casearia	Mafrica
Country	Italy	Spain
Company	CSP-F Solar	Aira Termosolar
Year	2015	2012
Collector model	fresnel collector	fresnel collector
Gross collector area (m^2)	995	2800
Collector opening area (m^2)	995	
Installed thermal power (kWth)	470	1600
HTF	Steam	Water
Storage	Without storage	
Conventional boiler	Steam boiler	
Fuel	Fuel oil	
Process	Cheese production	
Operating unit	other process heat	other process heat
Integration point	Supply line heating	Process medium heating
Process temperature (°C)	200 y 12 bar	
Collector temperature (°C)	200	
Investment (€)	140,000	875,000
Subsidies	260,000	30 %
Cost per gross area (€/m^2)	**140.7**	**312.5**
Solar fraction (%)	35	
Cost of fuel replaced (€/MWh fuel)	70	
Annual delivery of useful solar heat (MWh)	500	
Annual useful solar heat delivery per area (MWh/m^2)	0.5	

Table 6
Price update according to the evolution indicated by IRENA (LFC).

Surface area Solar field (m^2)	Cost per surface area (€/m^2)	Cost per updated surface area (€/m^2)
2880 (year 2021)	259.50	259.50
2800 (year 2012)	312.50	146.88
995 (year 2015)	402.01	276.10

Table 7
Investment and operating, maintenance and substitution costs by technology.

solar field size	Surface collectors (m^2)	C_I	C_{OMS} (%C_I)
	Costs PTC technology		
Medium	50–2000 m^2	360.90	5.60 %
Large	>2000 m^2	203.97	4.80 %
	Costs LFC technology		
Medium	50–2000 m^2	276.10	5.30 %
Large	>2000 m^2	203.19	4.60 %

For this reason, the average values considered in this study work was the average of the updated prices of both manufacturers (Inventive Power: 118.66 €/m^2; NEP Solar: 621.15 €/m^2) and the cost of installation of the updated studies, differentiating between the two price ranges based on the size of the solar collector field:

- Medium size (50 – 2000 m^2): 360.90 €/m^2.
- Large size (>2000 m^2): 203.97 €/m^2.

b) *Linear Fresnel Collector Technology (LFC)*

As for the previous technology, the following systems were found in the SHIP systems database [35], for which the price per m^2 of the gross LFC collector area was determined. This price refers to turnkey projects, including solar collectors, piping, support construction, storage, design, and commissioning, and excludes the VAT (Table 5).

For these systems, the same effect is reflected in relation to the economies of scale; for the smaller ones, a higher price is observed. It must also be considered that the manufacturer that implemented the smaller installation did so three years later, when the price was supposed to have reduced, which further intensified the economy of the scale factor. The prices obtained from the manufacturer considered for this study, namely Solatom, are shown in the first row:

Surface area Solar field (m^2)	Initial investment (€)	Cost per surface (€/m^2)
2880	747,369	259.50
2800	875,000	312.50
995	400,000	402.01

According to IRENA [34], CSP costs have decreased by 47 % from 2010 to 2019, which is equivalent to 5.22 % per year (linear), applying this trend from the year in which the previous plants were commissioned (2012 and 2015, except for Solatom, whose data were obtained from a simulation carried out on 3 February 2021) (Table 6).

The following ranges are established for the PTC technology depending on the size of the collector field:

- Medium size (50 – 2000 m^2): 276.10 €/m^2.
- Large size (>2000 m^2): 203.19 €/m^2 (average of the values obtained).

Once the two technologies have been analysed, the summary table of costs, including those related to operation and maintenance (in which the costs of replacement or substitution are added), is as follows (Table 7):

3.2.2. *Cost of energy from conventional sources*

This difficulty arises from the high volatility of current energy markets due to the energy crisis aggravated by the conflict in Ukraine, in addition to the situation generated by the pandemic (Covid-19). It also depends on the wide variety of existing tariffs and alterations which, in a habitual manner and without the need for extreme political circumstances, evolve over time.

This study focuses on the conventional energy sources used in dairy sector plants consulted during fieldwork, which could be extrapolated to most industrial processes: natural gas, diesel, and fuel oil.

a) *Natural Gas*

Three possible future scenarios were considered by analysing the evolution that has taken place over the past ten years. As the prices in recent years have been decreasing (except for 2021 and 2022, owing to the energy crisis aggravated by the conflict in Ukraine), we propose to maintain this option and two others with positive growth rates:

- *Medium scenario:* The evolution of prices continues with the same trend until the anomalous situation that caused the 2021 energy crisis. In this case, the annual growth rate was calculated for the last decade, which is curiously negative (it varies depending on the consumption band in which we belong). The annual average obtained for the next 20 years was applied from the high price set for the first half of 2021, because it was not possible to maintain the disproportionate growth trend of the last year.
- *Bullish scenario:* Price development is considered bullish (an unlikely scenario considering the starting price set for the first half of 2021), with a growth rate equivalent to half of the negative rate but with a positive value.
- *Very bullish scenario*: The price evolution assumes a growth rate whose value will double the negative growth rate in the medium scenario.

The methodology used is the one used from 2007 onwards which has been modified to cope with the liberalisation of the energy gas markets; the reference consumers are distributed in the following bands of annual consumption:

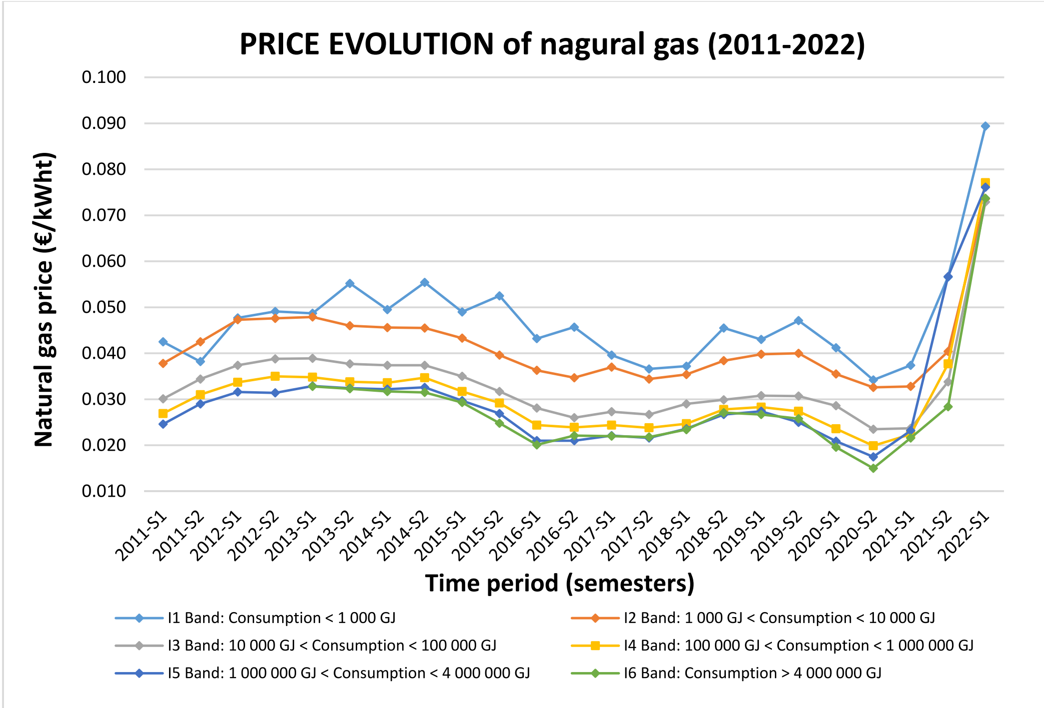

Fig. 11. Price evolution of natural gas (2011–2022).

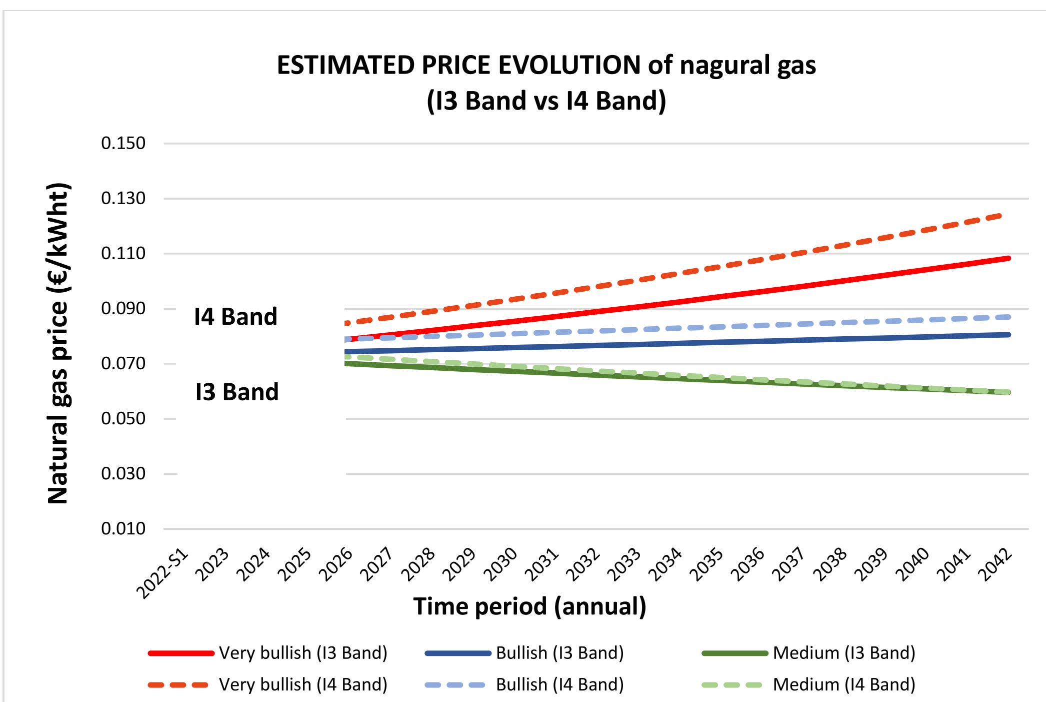

Fig. 12. Estimated price evolution of natural gas (2022–2042). Band-I3 vs Band-I4.

- I1 Band: annual consumption below 1.000 GJ.
- I2 Band: annual consumption between 1 000 and 10 000 GJ.
- I3 Band: annual consumption between 10 000 and 100 000 GJ.
- I4 Band: annual consumption between 100 000 and 1 000 000 GJ.
- I5 Band: annual consumption between 1 000 000 and 4 000 000 GJ.
- I6 Band: annual consumption above 4 000 000 GJ (voluntary).

Prices are collected from the Eurostat platform [38] considering three levels of taxation:

- prices without taxes and levies.
- prices without VAT and other recoverable taxes.
- prices with all taxes, levies and VAT.

To analyse the three possible future scenarios, prices without VAT and other recoverable taxes were considered, as well as those bands that

Table 8
Estimated prices of natural gas (2022–2042). Non-domestic sector.

Estimated prices of natural gas (2022–2042). Industrial sector.						
Type of consumption	Scenario	Price (€/kWh$_t$)				
		2022	2027	2032	2037	2042
I3 Band	Medium	0.0729	0.0693	0.0659	0.0627	0.0596
	Bullish	0.0729	0.0747	0.0766	0.0786	0.0805
	Very bullish	0.0729	0.0805	0.0889	0.0981	0.1083
I4 Band	Medium	0.0771	0.0717	0.0674	0.0634	0.0597
	Bullish	0.0771	0.0795	0.0819	0.0844	0.0870
	Very bullish	0.0771	0.0869	0.0979	0.1104	0.1244

reflected the most representative consumption of the industrial plants in the dairy sector referenced in the fieldwork, since, in this way, we would adjust better to the comparative reality in which we find ourselves immersed.

Of the 13 plants that used natural gas as conventional thermal energy, one used the I2 Band, seven used the I3 Band, and five used the I4 Band; therefore, we selected the I3 and I4 Bands as the most representative (Figs. 11,12).

The following table summarises the evolution of prices depending on the scenario and consumption band considered (Table 8).

b) *Diesel oil and fuel oil*

Oil is a valuable resource, given the dependence of most of the industrial sector on it. However, it is one of the most volatile commodities due to its susceptibility to geopolitical events. In addition, many of the world's most important reserves are located in unstable regions, such as the Middle East, Africa, and some parts of South America, where oil prices are in constant flux.

The most important factor influencing oil prices is the relationship between supply and demand. For this purpose, OPEC, which consists of 14 exporting countries, regulates prices by controlling supply. In 2018, OPEC countries limited their production to 39 million barrels of crude oil per day, which is more than one-third of daily global crude oil production [39].

The prices, including duties and taxes, were obtained from the Oil Bulletin platform [40], where they have been published since 2005 for all European Union countries. VAT is excluded only in the case of fuel oil; therefore, in order to use a single comparative criterion -the one used for natural gas- VAT will have to be deducted from the prices provided by Oil Bulletin (which currently amounts to 21 %, a tax that will be extrapolated in future scenarios assuming that it remains constant, despite being aware that in the past there have been small variations, which will be considered, such as in the period 01/07/2010 to 01/12/2012 when the applicable VAT was 18 % for Spain, being 21 % from that date onwards).

To make the price forecast for the next 20 years for both diesel and fuel oil, the projection will be resolved by generating a trend line from the known data, determining the rate that best fits owing to the number of external factors that would influence the value of the price of oil derivatives. The available fits for obtaining such a trend line are exponential, linear, logarithmic, polynomial, potential, and moving averages. The most appropriate type was selected based on the similarity index between the actual and projected data. Three very conservative scenarios are considered, as the current geopolitical and energy situation are both sufficiently complex such that the evolution of prices would not be moderate, which would further benefit renewable technologies by improving the viability of their integration into the industrial sector (Figs. 13,14):

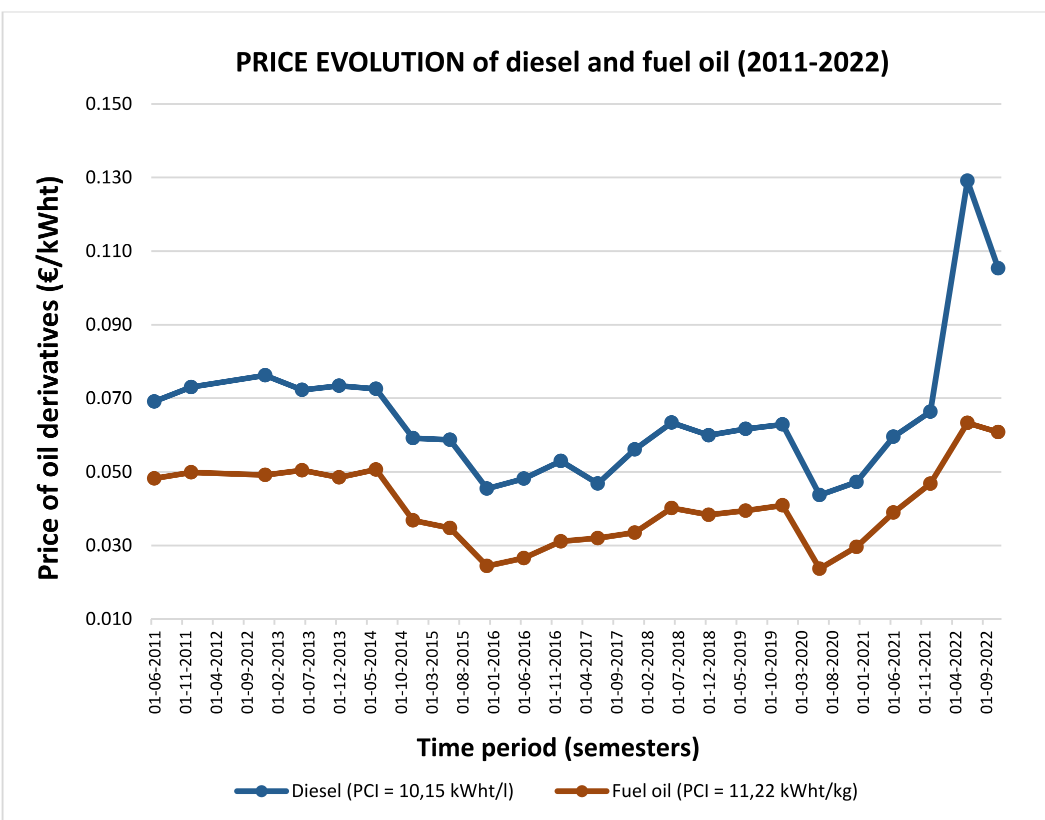

Fig. 13. Price evolution of diesel and fuel oil over the last decade (2011–2022).

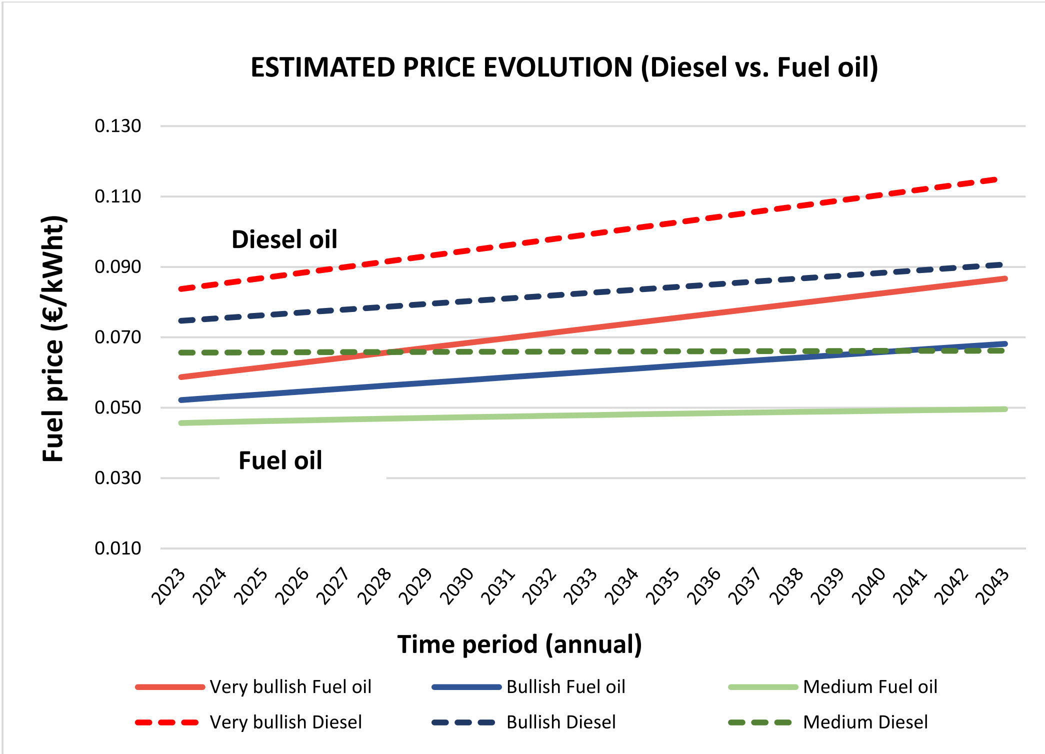

Fig. 14. Estimated price evolution of diesel oil vs. fuel oil (2023–2043).

Table 9
Table of Estimated prices of diesel and fuel oil (2022–2042).

Estimated prices of diesel and fuel oil (2022–2042)						
Fuel type	Scenario	Price (€/kWh$_t$)				
		2022	2027	2032	2037	2042
Diesel oil	Medium	0.1053	0.0658	0.0659	0.0661	0.0662
	Bullish	0.1053	0.0779	0.0819	0.0859	0.0899
	Very bullish	0.1053	0.0900	0.0979	0.1057	0.1136
Fuel oil	Medium	0.0608	0.0467	0.0477	0.0486	0.0494
	Bullish	0.0608	0.0555	0.0595	0.0635	0.0674
	Very bullish	0.0608	0.0643	0.0713	0.0783	0.0853

- *Medium scenario:* The evolution of prices continues with the same trend, considering the values of the last decade, that is, since December 2012, for which the logarithmic trend line was used (for fuel oil, the values from December 2014 are used to compensate for the fact that its increase in the previous year was not as rapid as for diesel).
- *Bullish scenario:* The evolution of prices is considered bullish, with a growth trend line that is linear for diesel since December 2012, and for fuel oil, it is the average of very bullish and medium scenarios.
- *Very bullish scenario:* Price development is equal to the linear trend line for fuel oil (considering data from December 2014 for the reason previously explained) and the sum of the difference between the bullish and average scenarios and the value of the bullish scenario for diesel.

In contrast to natural gas, for diesel and fuel oil, the period 2023–2043 is represented, since the price in 2022 increased in relation to the trend of the last decade. It was omitted from the graphical representation but considered in the calculations. The following table summarises the evolution of prices based on scenario and fuel type (Table 9).

Table 10
Locations of the dairy sector plants analysed.

COMPANY – Industrial Plant	Latitude (°)	Longitude (°)	Altitude (m)	Climate zone
1. Coreses (Zamora)	41.52423	−5,0.0093	645	D2
2. Morales del Vino (Zamora)	41.46344	−5.73202	697	D2
3. Fresno de la Ribera (Zamora)	41.53400	−5.57193	658	D2
4. Zamora	41.51679	−5.74098	652	D2
5. Baltanás (Palencia)	41.94476	−4.24223	780	D1
6. Coreses (Zamora)	41.52814	−5.64512	643	D2
7. Soria	41.75592	−2.46606	1063	E1
8. Santa Cristina de la Polvorosa (Zamora)	41.99365	−5.72178	734	D2
9. Candelaria (Santa Cruz de Tenerife)	28.34316	−16.37273	72	A3
10. Peñafiel (Valladolid)	41.59445	−4,12305	754	D2
11. Villarrobledo (Albacete)	39.27946	−2.59095	724	D3
12. Granada	37.17826	−3.64043	738	C3
13. Mollerusa (Lleida)	41.63100	0.90288	250	D3
14. Nadela (Lugo)	42.97278	−7.51078	510	E1
15. Villalba (Lugo)	43.28764	−7.64907	480	D1
16. Guadalajara	40.66453	−3.18033	708	D3
17. León	42.57101	−5.57138	837	E1

3.3. *Procedure for obtaining results*

3.3.1. *Location selection (climate zone)*

The potential for thermal energy production using medium-temperature concentration technologies depends on the location. Therefore, the locations of the plants in the dairy sector were analysed by selecting those that provided the most representative results in the national territory (Spain).

The Technical Building Code establishes in its Basic Document DB HE “Energy Saving” [41], Section HE 1 “Limitation of energy demand”,

Table 11
Locations selected as representative climate zones.

COMPANY – Industrial Plant	Latitude (°)	Longitude (°)	Altitude (m)	Climate zone
1. Coreses (ZAMORA)	41.52423	−5.60093	645	D2
5. Baltanás (PALENCIA)	41.94476	−4.24223	780	D1
7. SORIA	41.75592	−2.46606	1063	E1
9. Candelaria (SANTA CRUZ DE TENERIFE)	28.34316	−16.37273	72	A3
12. GRANADA	37.17826	−3.64043	738	C3
13. Mollerusa (LLEIDA)	41.63100	0.90288	250	D3
15. Villalba (LUGO)	43.28764	−7.64907	480	D1
Unknown (ALICANTE)	38.34109	−0.55921	5	B4

Annex B “Climatic zones”, the zones into which the national territory is divided, identifying them by a letter (climatic severity in winter) and a number (climatic severity in summer).

The locations of the plants (industrial processes in the dairy sector) analysed are as follows (Table 10):

3.3.2. Estimation of the solar resource

Different existing databases provide daily monthly average values of global horizontal radiation, that is, the average daily radiation (direct + diffused + solar albedo) for each month of the year. This value is known as the Typical Meteorological Year (TMY) and is made up of 8760 values (representing the 8760 h in a year) for each of the climatological variables under study (radiation, ambient temperature, humidity, wind speed, etc.). To generate a TMY, it is necessary to evaluate the solar resource monthly for at least 10 years, with hourly values. Thus, the monthly values for the year that best fit the average of the period considered would make up that month for the TMY. In other words, the representative meteorological year is composed of actual hourly values from different years (January 2013, February 2018, and March 2004).

The radiometric and meteorological variables considered are normal direct irradiance, global radiation, and mean outdoor temperature (minimum and maximum values), although the program’s database

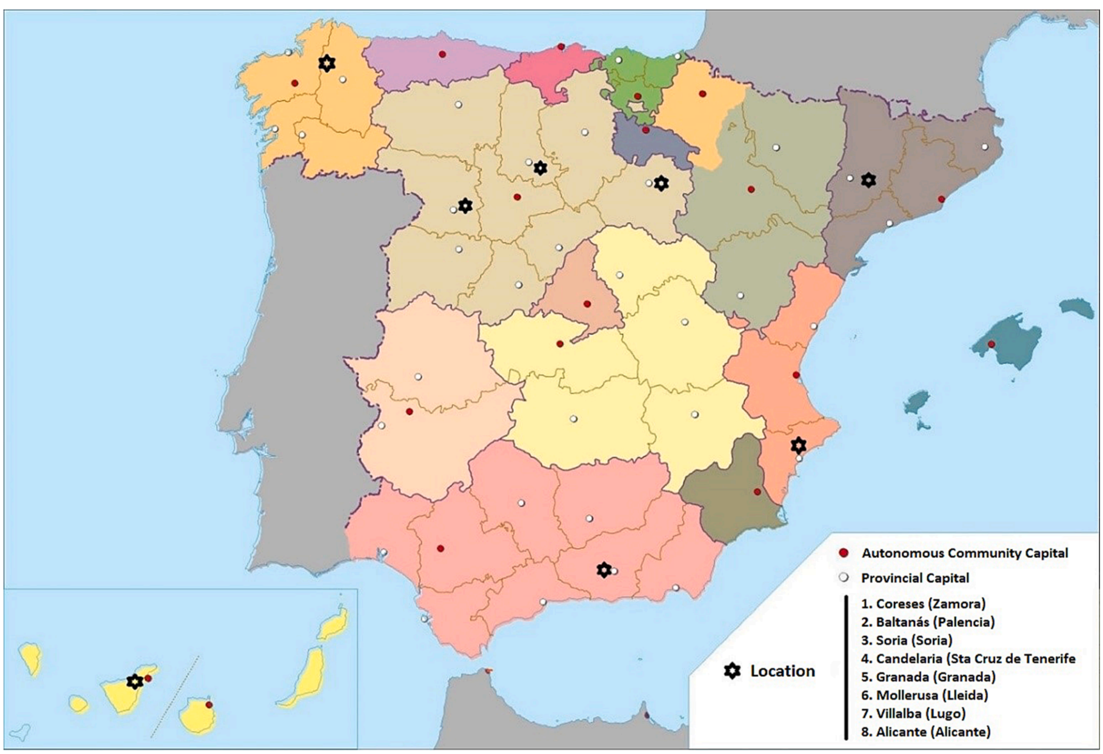

Fig. 15. Map of selected locations.

Table 12
Ambient temperature (minimum, maximum, monthly and annual average values) [49].

	Ambient temperature - monthly and annual average (°C)												
Location	**Annual**	**Ene**	**Feb**	**Mar**	**Abr**	**May**	**Jun**	**Jul**	**Ago**	**Sep**	**Oct**	**Nov**	**Dic**
Coreses (Zamora)	12,6	3,9	5,2	8,5	10,9	15,1	19,8	22,4	22,1	18,1	13,4	7,4	4,5
Baltanás (Palencia)	12,5	3,6	5,0	8,4	10,7	14,9	19,7	22,4	22,1	18,1	13,3	7,1	4,3
Soria (Soria)	12,3	4,0	5,1	9,1	10,1	14,4	19,9	22,0	21,6	17,1	12,6	6,5	4,3
Candelaria (Santa Cruz de Tenerife)	21,3	18,2	18,4	19,2	19,4	20,8	22,5	24,3	25,0	24,2	23,4	20,8	19,3
Granada (Granada)	15,7	6,0	7,6	10,9	13,8	18,4	23,7	26,7	26,2	21,1	16,6	9,8	6,7
Mollerusa (Lleida)	15,8	5,2	7,4	11,8	14,9	19,2	24,1	26,7	26,1	21,5	17,0	9,9	5,4
Villalba (Lugo)	12,5	7,5	7,6	9,6	10,8	13,3	16,3	18,1	18,4	16,7	14,0	9,7	8,2
Alicante (Alicante)	18,5	11,4	11,6	14,0	16,0	19,5	23,7	27,1	27,5	23,9	20,3	14,8	12,2

Table 13
Global radiation - monthly and annual accumulated (kWh/m²) [49].

Global radiation - monthly and annual accumulated (kWh/m²)													
Location	**Annual**	**Ene**	**Feb**	**Mar**	**Abr**	**May**	**Jun**	**Jul**	**Ago**	**Sep**	**Oct**	**Nov**	**Dic**
Coreses (Zamora)	1688,0	55,8	82,6	136,0	167,0	208,0	223,0	237,0	207,0	154,0	105,0	64,8	46,9
Baltanás (Palencia)	1629,0	52,9	75,9	129,0	161,0	200,0	211,0	227,0	206,0	153,0	104,0	61,9	46,8
Soria (Soria)	1568,0	51,8	74,3	127,0	152,0	191,0	217,0	222,0	193,0	141,0	94,8	58,6	45,2
Candelaria (Santa Cruz de Tenerife)	1846,0	99,0	114,0	154,0	179,0	205,0	208,0	219,0	199,0	149,0	126,0	98,5	95,1
Granada (Granada)	1841,0	79,4	93,2	143,0	175,0	214,0	234,0	244,0	215,0	164,0	122,0	84,7	74,1
Mollerusa (Lleida)	1656,0	56,6	84,8	138,0	166,0	204,0	219,0	226,0	197,0	147,0	105,0	64,4	48,4
Villalba (Lugo)	1264,0	43,9	64,1	107,0	132,0	159,0	158,0	160,0	150,0	117,0	83,8	50,3	40,9
Alicante (Alicante)	1749,0	78,0	92,0	142,0	171,0	210,0	223,0	225,0	197,0	150,0	115,0	78,8	67,2

Table 14
Normal direct irradiation - monthly and yearly accumulated (kWh/m²) [49].

Normal direct irradiation - monthly and yearly accumulated (kWh/m²)													
Location	**Annual**	**Ene**	**Feb**	**Mar**	**Abr**	**May**	**Jun**	**Jul**	**Ago**	**Sep**	**Oct**	**Nov**	**Dic**
Coreses (Zamora)	2098,0	87,2	119,0	170,0	187,0	225,0	241,0	276,0	246,0	206,0	155,0	107,0	79,6
Baltanás (Palencia)	1999,0	90,0	96,3	167,0	172,0	206,0	227,0	257,0	258,0	196,0	157,0	100,0	72,3
Soria (Soria)	1839,0	78,5	98,9	151,0	152,0	193,0	231,0	249,0	223,0	180,0	130,0	82,9	71,7
Candelaria (Santa Cruz de Tenerife)	1836,0	129,0	133,0	139,0	170,0	191,0	192,0	201,0	180,0	128,0	122,0	117,0	133,0
Granada (Granada)	2198,0	133,0	117,0	170,0	172,0	215,0	245,0	273,0	244,0	204,0	161,0	139,0	125,0
Mollerusa (Lleida)	1954,0	94,7	129,0	179,0	167,0	206,0	215,0	240,0	210,0	184,0	148,0	102,0	76,9
Villalba (Lugo)	1227,0	61,6	72,5	112,0	113,0	128,0	120,0	130,0	130,0	112,0	112,0	72,3	64,8
Alicante (Alicante)	1960,0	131,0	125,0	165,0	174,0	203,0	211,0	222,0	189,0	166,0	144,0	118,0	112,0

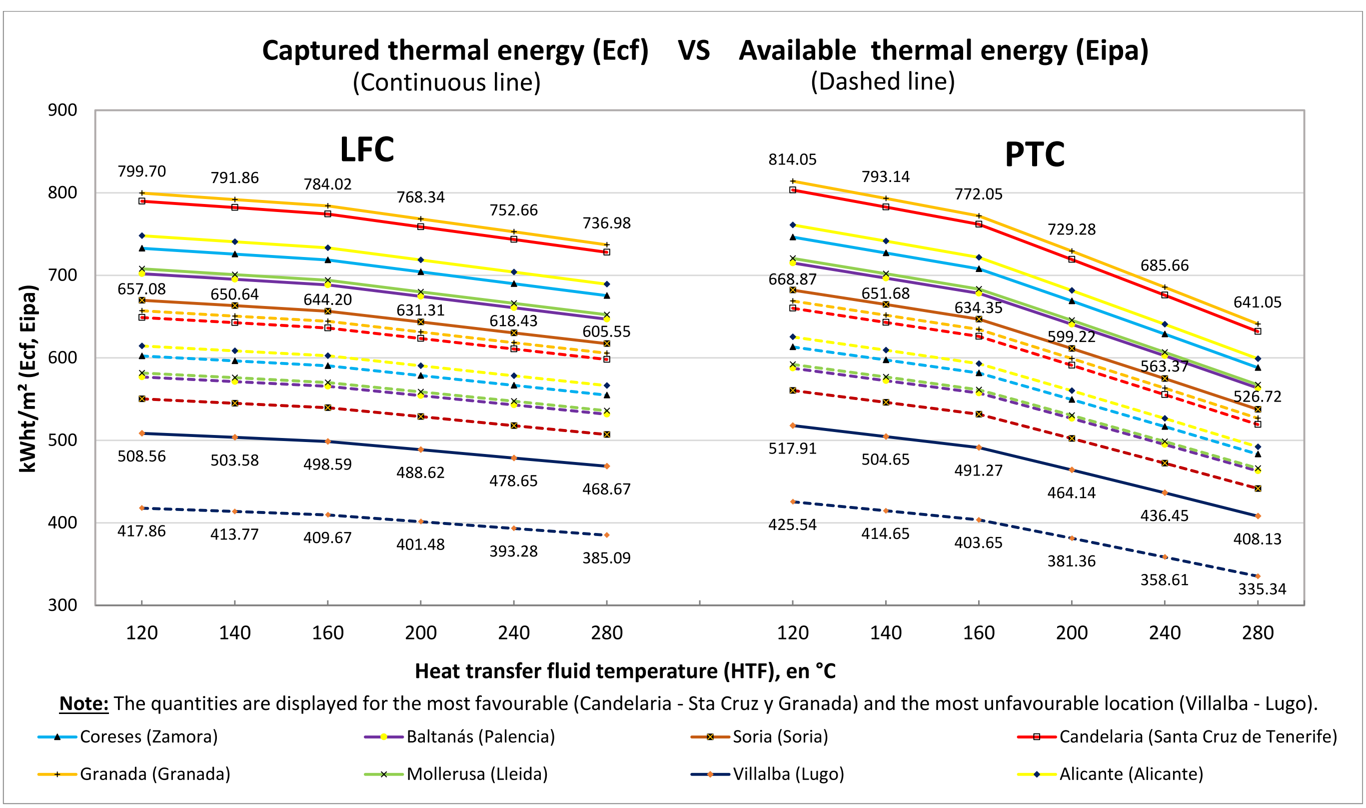

Fig. 16. E_{cf} VS. E_{IPA}.

included other values, such as diffused radiation, air humidity, wind speed, and thermal radiation.

The database could have been used according to the Meteonorm 7.2 software, which is linked to Polysun 12.0. However, it was decided to use the "web service" that this tool incorporates, since it receives the meteorological data of the location through the internet from the Meteonorm web service. This aspect is important, because in this way, the exact data of the locations is obtained from their coordinates.

3.3.3. Estimation of the thermal energy captured at the output of the solar collector field

To develop this section, it is necessary to differentiate between a series of concepts, such as solar radiation, irradiance, irradiation, direct irradiance, direct normal irradiance, direct horizontal irradiance, diffuse

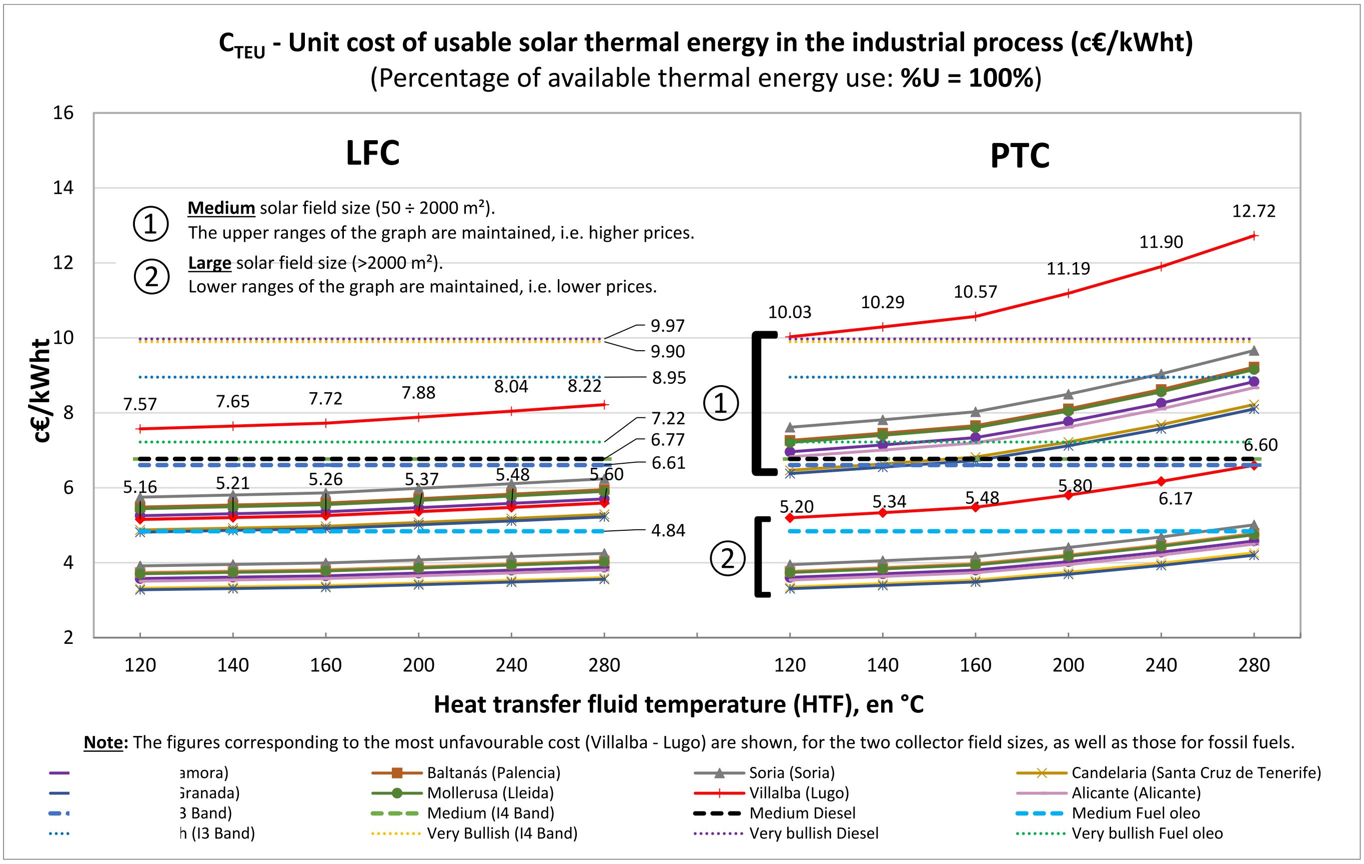

Fig. 17. C_{TEU}, considering a %U = 100 %, for the two technologies studied (LFC and PTC), and the two plant sizes (medium and large).

irradiance, and global irradiance [42].

The thermal energy generated by the solar collector field is quantified for each location and thermal level required, depending on the solar technology used.

For **LFC** technology, the following expression [43] is used to quantify the thermal energy captured in the collector field:

$$E_{cf} = \sum_{t=i}^{f} I_t \cdot \eta_{cf} \tag{8}$$

The incident solar irradiance is equivalent to the normal direct irradiance [30].

The thermal energy captured at the collector field output for **PTC** is determined using the energy balance described in Section 3.1.3., where the performance of this technology was characterised. Therefore, the thermal energy generated in the solar collector field during the representative year is

$$\boldsymbol{E_{cf}} = \sum_{t=i}^{f} \boldsymbol{E_t} \tag{9}$$

It is important to note that E_{cc} is different from the E_{DPI}, as there are thermal losses both in the external heat exchanger and the storage tank, and in the primary and secondary circuits (pipes), which depend on multiple factors, such as the type of insulation. Therefore, the energy available in industrial processes corresponds to the following expression [44]:

$$E_{IPA} = \sum_{t=i}^{f} E_{cf_t} \cdot \eta_{ehe} \cdot \eta_{tank} \cdot \eta_{cond} \tag{10}$$

where:

- η_{ehe}: external heat exchanger efficiency (90 %) [45].
- η_{tank}: tank efficiency (90 %) [46].
- η_{cond}: conduit efficiency (primary and secondary circuit pipes). For this the order of magnitude established for thermal installations in buildings is be used as an order of magnitude, not exceed 4 % of the maximum power transported [47]. for which it would be necessary to calculate the insulation required to comply with the aforementioned restriction. In this case what concerns us is that, when working at much higher temperatures, this value could be increased to 5 % so that the efficiency of the pipes would reach 95 %.

The efficiencies of the exchanger and the tank, with data from the references detailed above from the years 2012 and 2017, have been updated, going from 90 % to 92 % after consulting different manufacturers via telephone. These values depend on the type of exchanger (or tank) and working conditions. However, there are dimensions and flow rates that optimise the system, reaching the previously mentioned values. An exhaustive calculation would have to be carried out depending on the type of installation to determine these performances.

3.3.4. Estimation of the unit cost of solar thermal energy

To determine the unit cost of the thermal energy generated by a system that uses medium-temperature solar concentration technologies, it is necessary to know the thermal energy used by the industrial process and the costs associated with it over a given period of time. It is necessary to clarify that the energy used during the process is not related to the available thermal energy, as we are referring to the energy that is actually used in industrial processes. The expression [44] for use is

$$E_{UIP} = E_{IPA} \cdot \%U \cdot N \tag{11}$$

Two assumptions shall be made for the value of $\%U$: 100 % and 70 %. Now, it is necessary to estimate the cost of the useful life of the

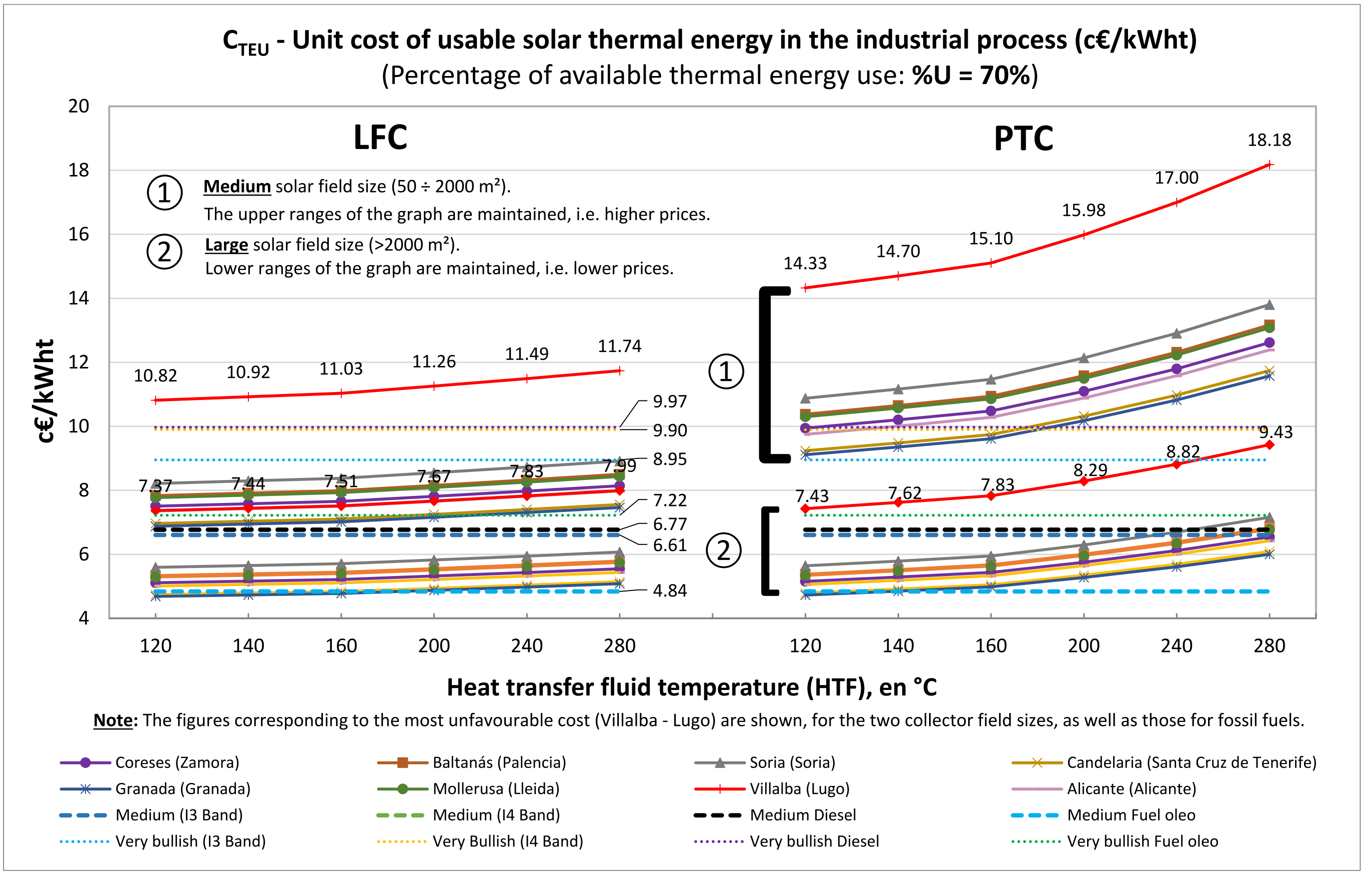

Fig. 18. Cost E_{UIP}, considering a %U = 70 %, for the two technologies studied (LFC and PTC), and the two plant sizes (medium and large).

thermal installation, for which it is essential to specify the annual investment and operation and maintenance costs, $\%C_{OMS}$, (the latter would include those corresponding to the required replacements or replacements), as indicated in Section 3.2.1. As the C_{OMS} is referenced as a percentage of investment costs, the CPI should be applied over the estimated period (20 years). For this purpose, the following expression is used [44]:

$$C_{UL} = C_I + \left(1 + \%C_{OMS} \cdot \sum_{i=0}^{19} \%CPI^i\right) \tag{12}$$

To determine the average CPI, the values corresponding to the last 15 years have been used [48]; considering a time interval of 22 years, the average CPI value was 2.31 %, and if the last 12 years were considered, it would be reduced to 1.87 %. Thus, using a time period of 17 years would provide a value that would coincide, approximately, with the average value of the two previous periods, 2.03 %.

Therefore, the unit cost of solar thermal energy can be adjusted using the following expression:

$$C_{TEU} = \frac{C_{UL}}{E_{UIP}} \tag{13}$$

4. Results and discussion

4.1. Technical study

4.1.1. Location selection (climate zone)

The locations used for this research, as indicated in Section 3.3.1, are those that provide representative results. One site corresponding to climate zone B4 was added to account for all severities in both winter and summer (Table 11) (Fig. 15).

4.1.2. Estimation of the solar resource

Despite considering hourly meteorological and radiometric values for the calculation of the performance of the concentrating solar collectors, tables with the monthly and annual average data of ambient temperature, global radiation, and normal direct irradiation are shown below (Tables 12–14).

The above tables show that the annual average ambient temperature ranges from 12.3 °C in Soria to 21.3 °C in Candelaria (Santa Cruz de Tenerife), the annual accumulated global horizontal irradiation ranges from 1264 kWh/m^2 in Villalba (Lugo) to 1846 kWh/m^2 in Candelaria (Santa Cruz de Tenerife), and the annual accumulated direct normal irradiation ranges from 1227 kWh/m^2 in Villalba (Lugo) to 2198 kWh/m^2 in Granada.

4.1.3. Estimation of the thermal energy captured at the solar collector field output

The results obtained in the estimation of the E_{cf} for each of the selected technologies and locations based on the performance equations in Sections 3.1 and 3.3.3, are presented below.

In the synthesis of the results obtained for the estimation of the E_{cf} (continuous line), those relating to the E_{IPA} (discontinuous line) are also included, where the losses in different equipment (exchanger, tank, and pipes) were considered. This is also true for the six thermal levels of the T_{HTF}.

It can be seen how, in general, the E_{cf} decreases as the T_{HTF} increases, by approximately 42 % (LFC) and 40 % (PTC), for a T_{HTF} of 200 °C. It can be seen that for temperatures below 140 °C, PTC technology is slightly more efficient than LFC, but above 160 °C, the converse is true and this change in trend intensifies as the temperature increases. These variations are consistent and proportional to the collector efficiency curves. However, it is important to note that this is true exclusively for the

Table 15
Summary C_{TEU} (c€/kWh$_t$).

Technology	% U	Unit cost of usable solar thermal energy in the industrial process (c€/kWht) — Catchment area (collector field) — MEDIUM Size (50–2000 m^2) — Temperature of the heat transfer fluid (HTF), in °C: 120	140	160	200	240	280	LARGE Size (>2000 m^2): 120	140	160	200	240	280
LFC	100 %	4,82–7,57	4,86–7,65	4,91–7,72	5,01–7,88	5,12–8,04	5,22–8,22	3,28–5,16	3,31–5,21	3,35–5,26	3,41–5,37	3,48–5,48	3,56–5,60
	70 %	6,88–10,82	6,95–10,92	7,02–11,03	7,16–11,26	7,31–11,49	7,46–11,74	4,69–7,37	4,73–7,44	4,78–7,51	4,88–7,67	4,98–7,83	5,08–7,99
PTC	100 %	6,38–10,03	6,55–10,29	6,73–10,57	7,12–11,19	7,57–11,90	8,10–12,72	3,31–5,20	3,40–5,34	3,49–5,48	3,69–5,80	3,93–6,17	4,20–6,60
	70 %	9,11–14,33	9,35–14,70	9,61–15,10	10,17–15,98	10,82–17,00	11,57–18,18	4,73–7,43	4,85–7,62	4,98–7,83	5,28–8,29	5,61–8,82	6,00–9,43

Table 16
Summary cost of thermal energy from conventional energy sources (c€/kWh$_t$).

Conventional energy source		Medium Scenario 2022	Medium Scenario 2042	Bullish Scenario 2022	Bullish Scenario 2042	Very bullish Scenario 2022	Very bullish Scenario 2042
Natural Gas	I3 Band	7.29	5.96	7.29	8.05	7.29	10.83
	I4 Band	7.71	5.97	7.71	8.70	7.71	12.44
Diésel		10.53	6.62	10.53	8.99	10.53	11.36
Fuel Oil		6.08	4.94	6.08	6.74	6.08	8.53

Thermal energy cost from conventional sources (c€/kWh$_t$)

medium-temperature concentration technology models analysed and cannot be generalised based on technology.

Logically, the values in the dotted line are in the lower ranges because they represent the E_{IPA} in which the aforementioned losses are included. All values are accumulated annually, displaying the figures corresponding to the most favourable location, Granada, and the most unfavourable location, Villalba (Lugo). Between the most favourable and most unfavourable locations, there is a difference in E_{cf} of 35.7 %, confirming the importance of the location (Fig. 16).

4.2. Economic study

A summary of the results is elaborated based on the estimation calculations of the C_{TEU} detailed in Section 3.3.4. based on the E_{UIP} and C_{UL}, considering a 20-year time horizon.

The structure in which the results are condensed is the same for each technology, including as variants the collector field surface (medium and large sizes, where the influence of the economy of scale concept will be noticeable), the T_{HTF} (which depends on the requirements of the industrial process), considering the same six thermal levels as for the technical study, and the %U (100 % or 70 %). The last parameter is related to the adjustment between the moment when energy is demanded by an industrial process and the instant at which it is generated in the solar collector field. This is precisely why the storage system is very important because it allows the demand profile to be adjusted to the process heat generation profile, thereby improving the flexibility of the system. This storage system can be used to increase the period of the day in which heat is supplied to compensate for variations in solar resources (total or partial absence of solar irradiation), providing the system with stability that it cannot otherwise have in areas with poor weather conditions.

A good design of the storage system allows us to take advantage of 100 % of the thermal energy available (Figs. 17,18).

The above figures are condensed in the following table, where the price ranges are reflected as a function of location, considering the technology, T_{HTF}, collector field size, and %U (Table 15):

Observing the table and figures above it can be stated that.

- The economy of the scale factor owing to the size of the collector solar field is key to the C_{TEU} regardless of the type of technology analysed.
- The same is true for the %U, which has a direct influence on the C_{TEU}, because the installation costs (C_I and C_{OMS}) remain unchanged.
- The impact of T_{HTF} varies depending on the technology analysed. However, the same pattern is maintained in all cases, as C_{TEU} increases with an increase in T_{HTF}.
- The technology with the lowest C_{TEU} is LFC (although for large sizes, there is hardly any difference). Although, for models with PTC technology from other manufacturers and larger sizes, aimed at obtaining $T_{HTF} > 250$ °C, even lower C_{TEU} can be obtained compared to LFC technology.
- For the particular case of Spain, the lowest C_{TEU} are for the location of Granada, and the highest for Villalba (Lugo).

Table 17
Total cost of energy demand in € (Two plant sizes and period of 20 years).

Scenario	Annual demand (GWh)	Natural Gas I3	Natural Gas I4	Diesel	Fuel oleo
Medium	60		81.663.454,94	81.482.921,11	57.952.430,27
	10	13.274.584,24		13.580.486,85	9.658.738,37
Bullish	60		98.035.676,21	99.684.000,00	71.441.215,14
	10	15.293.775,15		16.614.000,00	11.906.869,19
Very Bullish	60		117.222.611,88	117.885.078,89	84.930.000,00
	10	17.712.782,58		19.647.513,14	14.155.000,00

A summary of the results for the unit cost of thermal energy associated with conventional energy sources is presented below, considering the three scenarios detailed in Section 3.2.2. (Table 16).

Finally, the **annual net benefit** is determined in relation to the investment cost of the installation and considering its useful life (20 years) for all locations (making conclusions for the two extreme ones, Granada and Villalba (Lugo)), two plant sizes (60 GWh and 10 GWh), two solar fractions (15 % and 30 %), T_{HTF} = 200 °C, and the following initial boundary conditions or hypotheses.

- %U: 100 %.
- Payback period: 20 years.
- Conventional fuel price development: Medium scenario.
- The initial investment does not require pre-financing.

The total cost of demand (thermal energy consumed in the industrial process for the two plant sizes studied) over the period considered (useful life of 20 years), using only conventional fuels, increased to the following amounts (€) (Table 17,18):

It is important to highlight that although the locations that represent the two most extreme climatic zones have been shown, the meteorological and radiometric values of the rest are closer, to a greater extent, to the first of them (Granada). Therefore, the results of this study could be extrapolated to assess generic conclusions with respect to economic profitability. To do this, we only have to look at the values of both global radiation and normal direct irradiation for each of the locations, with Villalba (Lugo) being very distant from the rest, and the results for the latter being very different from those at the other locations considered.

The total cost of using conventional fuels (natural gas, diesel, and fuel oil) of the energy demand generated in the industrial process (dairy sector) is the same regardless of the location studied because the two plant sizes (demand of 60 GWh and 10 GWh) and the amortisation period are the same for all of them.

From the two tables above the following observations are made:

a) **Granada:**

1. *LFC Technology*

- For this case, regardless of the thermal demand of the installation (60 or 10 GWh), the system would always be economically profitable, although the difference between natural gas or diesel and fuel oil is important; since for the first two, the annual net benefit would be similar (10.50 % approximately), being more than double that of fuel oil (4.40 %).
- It may not have been economically profitable for fuel oil if, as the thermal demand in the industrial process decreased (i.e. for 10 GWh), the surface area of the collector field was reduced to less than 2000 m^2. In this situation, the economy of the scale factor is key to raising the cost of the initial investment in the execution of the installation, causing possible economic unfeasibility of the installation. It is verified that the collector field surfaces required for the thermal demand of 10 GWh/year reach 2376.01 m^2, higher than the 2000 m^2 referenced, confirming its economic profitability.
- The reason for maintaining the same percentage of net benefit for both solar field sizes is due to the fact that the greater investment due to the increase in the surface area of the collector field will result in greater production of energy, resulting in economic savings in the same proportion. In addition, for both size and solar fraction, collector fields with surface area greater than 2000 m^2 are still required, a limitation that would influence the price per m^2 of this technology owing to the economy of the scale factor.
- Using the annual net profit percentages associated with the different fuels, we obtain the period necessary to obtain a net profit equivalent to the investment cost of installation (Table 19):
- In other words, for all cases excluding fuel oil, in periods close to the middle of the useful life of the installation (approximately 10 years), we would obtain a net benefit equivalent to the investment cost, whereas for diesel, a period longer than the useful life would be necessary, approximately 23 years.

2. *PTC technology*

- With this technology, a somewhat lower annual net profit percentage is observed, as the cost of PTC technology is higher than that of LFC.
- The situations in which, using fuel oil, no net benefit could be obtained would correspond to the case of an annual thermal demand of 10 GWh and a solar fraction of 15 %, because the conditions for minimising the collector field surface area would be met but exceed 2000 m^2 (the limit for applying the economy of scale factor). It is verified that the collector field surface required for a thermal demand of 10 GWh/year is 2503.25 m^2, which is greater than the 2000 m^2 referenced.
- The savings obtained are very important for both sizes of the solar field and are nearly equal for natural gas and diesel. If we take as an example an annual demand of 60 GWh, these percentages would be 9.14 % and 9.10 %, respectively, which means a benefits of 182.80 % and 182.00 % of the initial investment over the 20 years. However, in the case of fuel oil, the net benefit is reduced to 3.34 % per year, i.e. 66.80 %, over the 20-year period.
- Using the annual net profit percentages associated with different fuels, we obtained the period necessary to obtain a net profit equal to the investment cost of the installation (Table 20):

Practically the same thing happens as for the previous technology (LFC technology); however, lower annual net benefits are obtained because the efficiency of PTC technology is lower for temperatures above 150 °C. The periods increased slightly: 11 years for the two natural gas tariffs and for diesel, and almost 30 years for fuel oil.

b) **Villalba (Lugo):**

1. *LFC Technology*

- In this case, regardless of the thermal demand of the installation (60 or 10 GWh), the system would always be economically profitable except for fuel oil.
- It is important to mention that for fuel oil, the annual net loss is only 1.06 % in relation to the investment cost of the installation, but the difference is so small that if the useful life is slightly extended, amortisation can be achieved. On the other hand, natural gas and diesel generate annual net profits, which are much lower than those obtained in Granada, because of poor weather conditions.
- In other words, the net benefit over the 20-year period considered, with LFC technology, for a T_{HTF} of 200 °C, would reach the following values:

▪ Natural Gas (I3): 50.00 % (2.50 % annual net benefits).

Table 18
Annual net benefit (payback period: 20 years) for Granada and Villalba (Lugo).

Technology	Annual demand in the process (GWh)	Solar fraction (%)	Annual Edpi (kWh/m²)	Collector field surface (m²)	Usable thermal E cost (c€/kWht)	Total usable solar energy cost (€)	Total savings (€) Natural Gas I3	Total savings (€) Natural Gas I4	Total savings (€) Diesel	Total savings (€) Fuel oleo	Annual net profit Natural Gas I3	Annual net profit Natural Gas I4	Annual net profit Diesel	Annual net profit Fuel Oil
Granada – Medium Scenario; %U = 100; Thtf = 200 °C														
LFC	60	15	631,31	14256,07	3,41	6143400,00		6106118,24	6079038,17	2549464,54		10,54 %	10,49 %	4,40 %
		30	631,31	28512,14	3,41	12286800,00		12212236,48	12158076,33	5098929,08		10,54 %	10,49 %	4,40 %
	10	15	631,31	2376,01	3,41	1023900,00	967287,64		1013173,03	424910,76	10,02 %		10,49 %	4,40 %
		30	631,31	4752,02	3,41	2047800,00	1934575,27		2026346,06	849821,51	10,02 %		10,49 %	4,40 %
PTC	60	15	599,22	15019,53	3,69	6647400,00		5602118,24	5575038,17	2045464,54		9,14 %	9,10 %	3,34 %
		30	599,22	30039,05	3,69	13294800,00		11204236,48	11150076,33	4090929,08		9,14 %	9,10 %	3,34 %
	10	15	599,22	2503,25	3,69	1107900,00	883287,64		929173,03	340910,76	8,65 %		9,10 %	3,34 %
		30	599,22	5006,51	3,69	2215800,00	1766575,27		1858346,06	681821,51	8,65 %		9,10 %	3,34 %
Villalba (Lugo) – Medium Scenario;%U = 100; Thtf = 200 °C														
LFC	60	15	401,48	22417,06	5,37	9660600,00		2588918,24	2561838,17	−967735,46		2,83 %	2,80 %	−1,06 %
		30	401,48	44834,11	5,37	19321200,00		5177836,48	5123676,33	−1935470,92		2,83 %	2,80 %	−1,06 %
	10	15	401,48	3736,18	5,37	1610100,00	381087,64		426973,03	−161289,24	2,50 %		2,80 %	−1,06 %
		30	401,48	7472,35	5,37	3220200,00	762175,27		853946,06	−322578,49	2,50 %		2,80 %	−1,06 %
PTC	60	15	381,36	23599,75	5,80	10443600,00		1805918,24	1778838,17	−1750735,46		1,88 %	1,85 %	−1,83 %
		30	381,36	47199,50	5,80	20887200,00		3611836,48	3557676,33	−3501470,92		1,88 %	1,85 %	−1,83 %
	10	15	381,36	3933,29	5,80	1740600,00	250587,64		296473,03	−291789,24	1,57 %		1,85 %	−1,83 %
		30	381,36	7866,58	5,80	3481200,00	501175,27		592946,06	−583578,49	1,57 %		1,85 %	−1,83 %

(Variables: Technology, annual thermal energy demand, and solar fraction). Medium Scenario. %U = 100. T_{HTF} = 200 °C.

Table 19
Time required to obtain a net benefit equivalent to the investment cost of the installation (years), for LFC technology in Grenada.

	Fuel			
	Natural Gas (I3)	Natural Gas (I4)	Diesel	Fuel oleo
Annual net profit	10.02 %	10.54 %	10.49 %	4.40 %
Time to obtain a net equivalent to the C_I (años)	9.98	9.49	9.53	22.73

Table 20
Time needed to obtain a net benefit equivalent to the investment cost of the installation (years), for PTC technology in Granada.

	Fuel			
	Natural Gas (I3)	Natural Gas (I4)	Diesel	Fuel oleo
Annual net profit	8.65 %	9.14 %	9.10 %	3.34 %
Time to obtain a net equivalent to the C_I (años)	11.56	10.94	10.99	29.94

- Natural Gas (I4): 56.60 % (2.80 % annual net benefits).
- Diesel: 56.00 % (2.80 % annual net benefits).

Approximately 36 years are required to obtain a net benefit equivalent to the C_I.

2. *PTC Technology*
   - Regarding the previous technology, regardless of the thermal demand of the installation (60 or 10 GWh), the system would always be economically profitable, except for fuel oil.
   - In this case, the annual net loss of fuel oil is 1.83 % in relation to the investment cost.
   - In other words, the net profit over the 20-year period considered for this PTC technology reaches the following value:
   - Natural Gas (I3): 31.40 %.
   - Natural Gas (I4): 37.60 %.
   - Diesel: 37.00 %.

   The annual net benefits are significantly lower as the yield of PTC technology for temperatures above 150 °C is lower, at 1.57 % (tariff I3 natural gas), 1.88 % (tariff I4 natural gas), and 1.85 % (diesel), longer periods to obtain a net benefit equivalent to the C_I.

As indicated previously, the other locations were similar to those in Granada. The following table summarises the **annual net benefits** for the three scenarios analysed (medium, bullish, and very bullish) and the two locations described. Only in the case of fuel oil in Villalba (Lugo) would there be a net loss in the medium scenario for both technologies, becoming profitable in the bullish and very bullish scenarios (Tables 21,22):

5. Future directions

Environmental criteria could be added, including a life cycle analysis (LCA), to verify the viability of the integration of medium-temperature SHIP systems in the industrial dairy sector, not only from a technical-energy and economic point of view. Other agri-food sectors could also be analysed, such as the processing, conservation, and production of meat products, which rank second in terms of existing SHIP systems worldwide. The same study could also be carried out with low-temperature solar technology (vacuum tube or flat plate and vacuum tube with compound parabolic concentrator) by checking its viability

Table 21
Annual net benefit equivalent to C_I for Granada (3 scenarios).

GRANADA Annual net profile		Fuel			
		Natural Gas (I3)	Natural Gas (I4)	Diesel	Fuel oleo
LFC	Medium Scenario	10.02 %	10.54 %	10.49 %	4.40 %
	Bullish Scenario	18.46 %	14.72 %	15.15 %	7.86 %
	Very Bullish Scenario	23.74 %	19.67 %	19.84 %	11.34 %
PTC	Medium Scenario	8.65 %	9.14 %	9.10 %	3.34 %
	Bullish Scenario	11.66 %	13.20 %	13.61 %	6.67 %
	Very Bullish Scenario	15.23 %	17.92 %	18.08 %	9.98 %

Table 22
Annual net benefit equivalent to C_I for Villalba (3 scenarios).

VILLALBA Annual net profile		Fuel			
		Natural Gas (I3)	Natural Gas (I4)	Diesel	Fuel oleo
LFC	Medium Scenario	2.50 %	2.86 %	2.80 %	**−1.06 %**
	Bullish Scenario	4.49 %	5.52 %	5.79 %	1.15 %
	Very Bullish Scenario	6.87 %	8.66 %	8.77 %	3.37 %
PTC	Medium Scenario	1.57 %	1.88 %	1.85 %	**−1.83 %**
	Bullish Scenario	3.46 %	4.44 %	4.70 %	0.28 %
	Very Bullish Scenario	5.73 %	7.44 %	7.55 %	2.39 %

considering the three selection criteria mentioned: technical-energy, economic, and environmental.

It could also be analysed as to what order of magnitude other variables would affect the efficiency of the systems, such as the accumulation volume, collector surface area (in this work, this was determined according to the solar fraction chosen and the size of the plant), setpoint temperature level, %*U*, demand profile, and the use of other heat transfer fluids.

In other words, there would be multiple options for future lines of research, being able to determine, with relative certainty, the advantages and disadvantages of using one or another technology, and confirming how these variables influence performance with the aim of obtaining concise conclusions that allow optimising the integration of these technologies in the industrial dairy sector according to the particular requirements of each plant, accelerating the implementation of renewable energy in the industrial sector, to achieve compliance with the SDS forecasts, for which economic support will be required from government authorities.

6. Conclusions

1. The thermal energy generated by both LFC and PTC technologies decreases as T_{HTF} increases, from an **average solar collector optical efficiency** of 63 % and 68 %, respectively for $T_{HTF} = 120\ ^\circ C$, to 42 % and 40 %, respectively, for temperatures of 200 °C. PTC technology is slightly more efficient than LFC technology up to temperatures of 140 °C. However, from 160 °C onwards, the converse is true, with the trend reversal intensifying as T_{HTF} increases. This is the case for the PTC and LFC concentration technology models analysed and cannot be extended to other models and manufacturers.
2. The **efficiency of the installation** (E_{cf}/energía demandada) depends on the installed collector surface (provided that the number of collectors connected in series remains constant). If we have batteries with a certain number of collectors connected in series and increase the number of batteries, for example, from 100 to 200, we would double the surface area, and therefore, the useful heat, which would also double the installation efficiency. However, if we increase the number of collectors in series, the thermal jump would be modified, which would influence the collector performance (as reflected in its performance curves, as the T_{HTF} would be higher); therefore, the efficiency of the installation, as less useful thermal energy, would be generated at the output of the collector field.
3. Multiple variables influence the $\boldsymbol{C_{TEU}}$, regardless of the technology being analysed. The *economy of scale factor* due to the size of the solar collector field is key, as is *%U*, because in the latter case, the installation costs (C_I y C_{OMS}) remain unchanged. The higher the %U, the greater the renewable energy used in the industrial process and, therefore, the lower the energy consumed from conventional sources. This fact ratifies the importance of adjusting the thermal energy demand profile in the industrial process with that of generation in the solar collector field, requiring a good design of the storage system that allows 100 % of the E_{cc} to be used.
4. Similarly, as the T_{HTF} increases, the C_{TEU} also increases slightly. As the T_{HTF} increases, the difference becomes more noticeable, with the LFC technology being more economical than the PTC for the collector models analysed. For large solar collector field sizes, this difference is negligible. This does not mean that for PTC technology models of other manufacturers and larger dimensions aimed at obtaining $T_{HTF} > 250\ ^\circ C$, even lower C_{TEU} can be obtained than that with LFC technology.
5. Both technologies perform similarly in all **locations** depending on the available solar resources. The location with the highest efficiency in the installation corresponds to Granada, passing through Candelaria (Santa Cruz de Tenerife), Alicante, Mollerusa (Lleida), Coreses (Zamora), Baltanás (Palencia) until reaching Villalba (Lugo), with a difference, between the most favourable and most unfavourable, of approximately 35.7 %, confirming the importance of the location of the installation. For the particular case of Spain, the **lowest** $\boldsymbol{C_{TEU}}$ is related to Granada and the **highest** to Villalba (Lugo).

CRediT authorship contribution statement

Rubén Rodríguez Rodrigo: Conceptualization, Data curation, Writing – original draft, Writing – review & editing, Visualization, Investigation, Validation, Formal analysis, Methodology. **Ricardo Díaz Martín:** Supervision. **Marcos Baranda Fernández:** Resources. **Jesús Ángel Román Gallego** Project administration, Software. **Carlos Mayo del Río:** Project administration, Software.

Declaration of competing interest

The authors declare that they have no known competing financial interests or personal relationships that could have appeared to influence the work reported in this paper.

Acknowledgments

This research did not receive any specific grant from funding agencies in the public, commercial, or not-for-profit sectors.

References

[1] BP, Statistical Review of World Energy 2022 | 71th edition, 2022. [Online]. Available: https://www.bp.com/en/global/corporate/energy-economics.html. [Accessed: 13-Nov-2022].
[2] International Energy Agency, Global energy review 2019, 2019. [Online]. Available: https://www.iea.org/reports/global-energy-review-2019. [Accessed: 13-Nov-2022].
[3] David Hodgson, T. Vass, P. Levi, P. Hugues, IEA reports industry, 2022. [Online]. Available: https://www.iea.org/reports/industry. [Accessed: 13-Nov-2022].
[4] International Energy Agency (IEA), Direct CO2 emissions from industry in the Net Zero Scenario, 2000-2030 – Charts – Data & Statistics - IEA, 2022. [Online]. Available: https://www.iea.org/data-and-statistics/charts/direct-co2-emissions-from-industry-in-the-net-zero-scenario-2000-2030. [Accessed: 29-Jan-2023].
[5] IRENA Coalition for Action, Companies in transition towards 100% renewables: Focus on heating and cooling, Abu Dhabi, 2021.
[6] B. Epp, Encouraging solar industrial heat market trends | Solarthermalworld, Solar thermal world, 2022. [Online]. Available: https://solarthermalworld.org/news/encouraging-trends-in-the-solar-industrial-heat-market-2021/. [Accessed: 29-Jan-2023].
[7] A. K. Sharma, C. Sharma, S. C. Mullick, T. C. Kandpal, Potential of solar industrial process heating in dairy industry in India and consequent carbon mitigation, J. Clean. Prod., 140(Part 2) (2017) 714–72.
[8] A. Allouhi, et al., Design optimization of a multi-temperature solar thermal heating system for an industrial process, Appl. Energy 206 (2017) 382–392.
[9] A.K. Sharma, C. Sharma, S.C. Mullick, T.C. Kandpal, Financial viability of solar industrial process heating and cost of carbon mitigation: A case of dairy industry in India, Sustain. Energy Technol. Assessments 27 (Jun. 2018) 1–8.
[10] A. Moerkerken, S. Duijndam, J. Blasch, P. van Beukering, A. Smit, Determinants of energy efficiency in the Dutch dairy sector: dilemmas for sustainability, J. Clean. Prod. 293 (Apr. 2021) 126095.
[11] S.H. Farjana, M.A.P. Mahmud, N. Huda, Solar process heat integration in lead mining process, Case Stud. Therm. Eng. 22 (Dec. 2020) 100768.
[12] O. May Tzuc, A. Bassam, L.J. Ricalde, O.A. Jaramillo, M. Flota-Bañuelos, M. A. Escalante Soberanis, Environmental-economic optimization for implementation of parabolic collectors in the industrial process heat generation: Case study of Mexico, J. Clean. Prod. 242 (Jan. 2020) 118538.
[13] E. S. T. I. F. ESTIF, Solar heat for industrial processes, 2017. [Online]. Available: http://solarheateurope.eu/project/solar-heat-industrial-process/. [Accessed: 08-Aug-2023].
[14] E. S. T. I. F. ESTIF, Solar Payback, 2021. [Online]. Available: https://www.solar-payback.com/technology/. [Accessed: 13-Aug-2022].
[15] B. Schmitt, Solar Proccess Heat depends on the conventional heating equipment, Solar & cooling programme (IEA), 2016. [Online]. Available: https://www.iea-shc.org/article?NewsID=116. [Accessed: 08-Dec-2019].
[16] B. Muster, et al., Integration Guideline, Integr. Guidel. Sol. Process Heat Prod. Adv. Appl. no. February (2015).
[17] UNE, UNE-EN ISO 9806:2020 Energía solar. Captadores solares térmico... Spain, 2020.
[18] Solar Keymark, Solarkeymark database collectors, 2023. [Online]. Available: https://solarkeymark.eu/database/. [Accessed: 23-Feb-2023].
[19] A. Hofer, et al., State of the art of performance evaluation methods for concentrating solar collectors, AIP Conf. Proc. 1734 (May 2016).
[20] STAGE-STE, Stage-STE Database, 2023. [Online]. Available: http://193.146.147.224/keydocuments/solar_collectors/index.php/SolarCollectors/.
[21] TRNSYS Software, TRNSYS V.18.03.0002, 2021. [Online]. Available: http://www.trnsys.com. [Accessed: 27-Apr-2021].
[22] COLSIM Software, COLSIM 0.63 (Collector Simulation Environment).
[23] INSEL Software, INSEL 8.2 (INtegrated Simulation Environment Language). [Online]. Available: https://www.insel.eu/de. [Accessed: 31-Jan-2021].
[24] Valentin-software, T*SOL 2018. [Online]. Available: https://valentin-software.com/en/products/tsol/#release-notes. [Accessed: 01-Feb-2021].
[25] DLR, GREENIUS 4.5.0, 2021. [Online]. Available: https://www.dlr.de/sf/en/desktopdefault.aspx/tabid-11688/20442_read-44865/index.php/get-freegreenius/. [Accessed: 02-Feb-2021].
[26] SAM Sofware, SAM (System Advisor Model), 2021. [Online]. Available: https://sam.nrel.gov/download/63-sam-2020-11-29-for-windows.html. [Accessed: 03-Feb-2021].
[27] AIGUASOL, TRANSOL, 2021. [Online]. Available: https://aiguasol.coop/es/project/software-para-el-diseno-optimizacion-y-gestion-energetica-de-sistemas-solares-termicos-transol/. [Accessed: 09-Feb-2021].
[28] SIMTECHNOLOGY, IPSEPRO, 2021. [Online]. Available: https://www.simtechnology.com/CMS/index.php/ipsepro. [Accessed: 09-Feb-2021].
[29] Velasolaris, Polysun 12.0, 2021. [Online]. Available: https://www.velasolaris.com/software/?lang=en. [Accessed: 02-Feb-2021].
[30] H. Schweiger, C. Vannoni, I. Pinedo Pascua, E. Facci, D. Baehrens, and M. Koch, Evaluación del Potencial de la Energía Solar Térmica en el Sector Industrial. Estudio técnico PER 2011-2020. Madrid, 2011.
[31] Solatom, Solatom, 2021. [Online]. Available: https://solatom.com/index/tecnologia/. [Accessed: 16-May-2022].
[32] V. Ruiz Hernández, M. A. Silva Pérez, and I. Lillo Bravo, La electricidad solar térmica, tan lejos, tan cerca., 1ª edición. Barcelona, 2009.
[33] Nep solar, Nep solar PolyTrough 1800, 2019. [Online]. Available: chrome-extension://oemmndcbldboiebfnladdacbdfmadadm/http://www.nep-solar.com/wp-content/uploads/2013/11/NEP-Solar-Polytrough1800_Datasheet.pdf. [Accessed: 17-May-2021].
[34] IRENA, Renewable power generation costs in 2019, Abu Dhabi (2020).
[35] Ship-plants.info, Solar Thermal Plants Database, 2021. [Online]. Available: http://ship-plants.info/solar-thermal-plants. [Accessed: 18-May-2022].
[36] C. Kutscher, M. Mehos, C. Turchi, G. Glatzmaier, T. Moss, Line-Focus Solar Power Plant Cost Reduction Plan (Milestone Report), Dec. 2010.
[37] R. Silva, M. Berenguel, M. Pérez, A. Fernández-Garcia, Thermo-economic design optimization of parabolic trough solar plants for industrial process heat applications with memetic algorithms, Appl. Energy 113 (2014) 603–614.
[38] Eurostat, Eurostat, 2023. [Online]. Available: https://ec.europa.eu/eurostat. [Accessed: 05-Jan-2023].
[39] IG España, Los 7 factores que afectan el precio del petróleo, 2021. [Online]. Available: https://www.ig.com/es/estrategias-de-trading/los-7-factores-que-afectan-el-precio-del-petroleo-190307#:~:text=El precio del petróleo en,del llamado %22oro negro%22.&text=El petróleo es una materia prima codiciada. [Accessed: 11-May-2021].
[40] European Commission, Weekly Oil Bulletin, 2023. [Online]. Available: https://energy.ec.europa.eu/data-and-analysis/weekly-oil-bulletin_en. [Accessed: 04-Jan-2023].
[41] M. y A. U. Ministerio de Transporte, Documento Básico HE Ahorro de Energía. Spain: Código Técnico de la Edificación, 2022.
[42] Ministerio de Industria Energía y Minas, Glosario de la Agencia Andaluza de la Energía, 2021. [Online]. Available: https://www.agenciaandaluzadelaenergia.es/Radiacion/glosario.php. [Accessed: 11-May-2021].
[43] UNE, UNE-EN 12975-2:2006 Sistemas solares térmicos y componentes. Captadores solares. Parte 2: Métodos de ensayo. Spain, 2006.
[44] R. Rodríguez Rodrigo, Technical-energetic, economic and environmental analysis of medium temperature concentrating solar power technologies for the dairy industry in Spain, Complutense University of Madrid, 2022.
[45] Z. Ma, G. Glatzmaier, C. Turchi, M. Wagner, Thermal Energy Storage Performance Metrics and Use in Thermal Energy Storage Design, ASES World Renewable Energy Forum Denver (2012) 6.
[46] S. Pintaldi, S. Sethuvenkatraman, S. White, G. Rosengarten, Energetic evaluation of thermal energy storage options for high efficiency solar cooling systems, Appl. Energy 188 (Feb. 2017) 160–177.
[47] Ministerio de la Presidencia, Real Decreto 1027/2007, de 20 de julio, por el que se aprueba el Reglamento de Instalaciones Térmicas en los Edificios. Spain, 2022.
[48] Instituto Nacional de Estadística, Instituto Nacional de Estadística de España, 2022. [Online]. Available: https://www.ine.es/. [Accessed: 21-May-2022].
[49] W. Service, Polysun 12.0. 2021.